Emissions of biogenic volatile organic compounds and subsequent photochemical production of secondary organic aerosol in mesocosm studies of temperate and tropical plant species

Kevin P. Wyche[1,2], Annette C. Ryan[3*], C. Nicholas Hewitt[3], M. Rami Alfarra[4,5], Gordon McFiggans[4], Timo Carr[1], Paul S. Monks[1], Kirsty L. Smallbone[2], Gerard Capes[5], Jacqueline F. Hamilton[6], Thomas A. M. Pugh[7], and A. Robert MacKenzie[8]

1. Department of Chemistry, University of Leicester, Leicester, LE1 7RH, UK

2. School of Environment and Technology, University of Brighton, Brighton, BN2 4GJ

3. Lancaster Environment Centre, Lancaster University, Lancaster, LA1 4YQ, UK

4. School of Earth, Atmospheric and Environmental Sciences, The University of Manchester, M13 9PL, UK

5. National Centre for Atmospheric Science, The University of Manchester, M13 9PL, UK

6. Dept. of Chemistry, University of York, York, YO10 5DD, UK

7. Karlsruhe Institute of Technology, IMK-IFU, Garmisch-Partenkirchen, Germany

8. Birmingham Institute of Forest Research, University of Birmingham, B15 2TT, UK

*For correspondence:
A. C. Ryan,
Lancaster Environment Centre,
Lancaster University,
Lancaster,
LA1 4YQ,
UK.

Tel: 01524 594 534
Email: a.ryan@lancaster.ac.uk

Abstract: Silver birch (*Betula pendula*) and three Southeast Asian tropical plant species (*Ficus cyathistipula, Ficus benjamina* and *Caryota millis*) from the pantropical fig and palm genera were grown in a purpose-built and environment-controlled whole-tree chamber. The volatile organic compounds emitted from these trees were characterised and fed into a linked photochemical reaction chamber where they underwent photooxidation under a range of controlled conditions (RH ~ 65 – 89 %, VOC/NO_x ~ 3 – 9 and NO_x ~ 2 ppbV). Both the gas phase and the aerosol phase of the reaction chamber were monitored in detail using a comprehensive suite of on-line and off-line, chemical and physical measurement techniques.

Silver birch was found to be a high monoterpene and sesquiterpene, but low isoprene emitter, and its emissions were observed to produce measureable amounts of SOA via both nucleation and condensation onto pre-existing seed aerosol (Y_{SOA} 26 – 39 %). In contrast, all three tropical species were found to be high isoprene emitters with trace emissions of monoterpenes and sesquiterpenes. In tropical plant experiments without seed aerosol there was no measurable SOA nucleation, but aerosol mass was shown to increase when seed aerosol was present. Although principally isoprene emitting, the aerosol mass produced from tropical fig was mostly consistent (i.e., in 78 out of 120 aerosol mass calculations using plausible parameter sets of various precursor specific yields) with condensation of photooxidation products of the minor VOCs co-emitted; no significant aerosol yield from condensation of isoprene oxidation products was required in the interpretations of the experimental results. This finding is in line with previous reports of organic aerosol loadings consistent with production from minor

biogenic VOCs co-emitted with isoprene in principally-isoprene emitting landscapes in Southeast Asia. Moreover, in general the amount of aerosol mass produced from the emissions of the principally-isoprene-emitting plants, was less than would be expected from published single-VOC experiments, if co-emitted species were solely responsible for the final SOA mass. Interpretation of the results obtained from the fig data sets, leaves room for a potential role for isoprene in inhibiting SOA formation under certain ambient atmospheric conditions, although instrumental and experimental constraints impose a level of caution in the interpretation of the results.

Concomitant gas and aerosol phase composition measurements also provide a detailed overview of numerous key oxidation mechanisms at work within the systems studied and their combined analysis provides insight into the nature of the SOA formed.

Keywords: Secondary organic aerosol, biogenic volatile organic compounds, BVOC, gas-aerosol partitioning, isoprene, monoterpenes, mesocosm

Introduction

Atmospheric aerosols change the radiative balance of the Earth through scattering and absorbing incident solar radiation (Kim and Ramanathan, 2008); they directly and indirectly affect the properties and formation of clouds, thus altering the hydrological cycle (Gunthe et al., 2009;Junkermann et al., 2009;Stevens and Feingold, 2009); and they may have an impact on the efficiency of plant photosynthesis (Mercado et al., 2009), thereby modifying the uptake of atmospheric carbon. Hence, aerosol particles affect the Earth's climate in several ways (as reviewed in Hallquist et al., 2009;IPCC, 2007;Isaksen et al., 2009;Carslaw et al., 2010) as well as having a detrimental impact on human health (e.g., Baltensperger et al., 2008).

A large fraction of the observed atmospheric aerosol composition is organic (Zhang et al., 2007). A primary organic component is emitted directly into the atmosphere from anthropogenic activities, such as biomass burning and fossil fuel combustion, or is emitted from natural sources, such as plant abrasion and the sea surface. Secondary aerosol particles are formed within the atmosphere by gas-to-particle conversion; those formed from gas-phase organic precursors are known as secondary organic aerosol (SOA) (e.g., Riipinen et al., 2012). There is considerable uncertainty surrounding the chemical transformation of anthropogenic and biogenic volatile organic compounds (AVOC and BVOC, respectively) from the gas phase to the aerosol phase and hence, considerable uncertainty in the global source of SOA (Hallquist et al., 2009;Donahue et al., 2009;Ng et al., 2006;Virtanen et al., 2010).

92 On a global scale, approximately 90 % of all volatile organic compound emissions
93 originate from biogenic sources (Guenther et al. 2012), with almost half of this being
94 emitted from tropical and subtropical forests. The ability of biogenic VOC to form
95 SOA is therefore of particular interest and potential importance. Globally, isoprene
96 (2-methyl-1,3-butadiene, C_5H_8) is the biogenic VOC with the largest mass emission
97 rate. It is estimated to account for about 50 % of BVOC emissions by mass (Guenther,
98 et al. 2012), but it is still uncertain how much it contributes to SOA formation (Karl et
99 al., 2009;Carlton et al., 2009).

100 Modelling, laboratory chamber experiments and field studies provide a range of
101 possible yields of SOA from isoprene, typically of the order 0.1 – 3 % by mass, with
102 some values reported as high as 5.5 % (van Donkelaar et al., 2007;Kleindienst et al.,
103 2009, 2007;Kroll et al., 2005, 2006;Claeys et al., 2004a;Edney et al., 2005;
104 Brégonzio-Rozier et al., 2014). SOA yields from the further oxidation of first and
105 subsequent generation isoprene oxidation products, such as methacrolein, are
106 estimated to be as much as 15 % (Rollins et al., 2009;Carlton et al., 2009;Claeys et
107 al., 2004b;Robinson et al., 2010). Recent work has highlighted that under low NO_x
108 conditions, SOA mass formed from isoprene oxidation could be influenced by the
109 acidity of pre-existing aerosol via the reactive uptake of certain key isoprene
110 oxidation products, namely isoprene epoxydiols (IEPOX; Surratt et al., 2010; Lin et
111 al., 2012). More recently, Nguyen et al. (2014) found that the "pH dependence for OA
112 formation from IEPOX was weak for AS particles". There is further evidence from
113 chamber studies using temperate tree species such as birch, spruce and pine that

114 isoprene may in fact suppress SOA formation from other VOC precursors, when
115 present (Kiendler-Scharr et al., 2009a;Kanawade et al., 2011). It should be noted at
116 this point that it is unclear in most cases how wall effects have been considered in the
117 production of such yield values and whether the treatments employed are adequate
118 such that the yields are comparable between chambers, or indeed between
119 experiments.

120 Here, we characterised the BVOC emissions from three south-east Asian tropical
121 plant species (*Ficus cyathistipula, Ficus benjamina* and *Caryota millis*) and in a series
122 of coupled plant growth chamber–atmospheric reaction chamber experiments, we
123 examined the ability of their oxidation products to contribute to SOA formation under
124 atmospherically relevant conditions. In order to provide a geographically and
125 chemically contrasting study, we replicated these experiments using common silver
126 birch (*Betula pendula*). Silver birch has previously been shown to contribute to the
127 formation of secondary organic aerosol via the emissions of mono- and sesquiterpenes
128 (e.g. Kiendler-Scharr et al., 2009a;2009b;Mentel et al., 2009). Seeded (ammonium
129 sulphate) and un-seeded experiments were carried out to allow studies of both fresh
130 nucleation and condensation onto pre-existing aerosol.

131 **Methods and materials**

132 ***2.1 Plant selection and pre-screening***

Three non-clonal specimens of common silver birch (*Betula pendula*), a monoterpene and isoprene emitting tree species; two species of fig (*Ficus benjamina* and *Ficus cyathistipula*), and one species of palm (*Caryota millis*), each approximately 1.5 m in height were used. Figs and palms are abundant in all tropical rainforests. We chose three species found in abundance throughout south and southeast Asia to be consistent with our field work (Hewitt et al., 2010a;MacKenzie et al., 2011). *Ficus benjamina* (Moraceae) is native to Malaysia and has previously been found to be a high isoprene emitter (0.03 – 8.7 μg C g^{-1} h^{-1}, potted and in soil) with emissions of the monoterpenes, limonene (0.02 μg C g^{-1} h^{-1}) and β-ocimene (1.8 – 2.5 μg C g^{-1} h^{-1}), and the sesquiterpenes β-caryophyllene and α-copaene (Carvalho et al., 2005;Geron et al., 2006). In addition, emissions of benzaldehyde (0.53 μg C g^{-1} h^{-1}) and acetaldehyde (69 μg C g^{-1} h^{-1}) from potted specimens have been detected (Carvalho et al., 2005). No previous data are available on the BVOC emissions from *Ficus cyathistipula* or *Caryota millis*. Proton transfer-reaction mass spectrometry (PTR-MS) and gas chromatography–mass spectrometry (GC-MS) screening, prior to the start of the coupled chamber experiments, confirmed that both species were high isoprene emitters with *Ficus cyathistipula* also emitting limonene, β-phellandrene, α-damascone and acetaldehyde. Analytical methods are described in detail in section 2.4.

2.2 Plant chamber design

153 A 4.7 m^3 plant chamber was constructed out of two rectangular Teflon bag sections
154 and a Teflon lid (0.05 mm FEP) (Adtech Polymer Engineering, UK), which were each
155 supported by frames built using 25 mm^2 box aluminium (Speed Frame, RS
156 Components, UK). The framework stood on a raised foil and Teflon covered marine
157 plywood base. PVC foam strips (RS Components, UK) ensured an airtight seal
158 between chamber sections. Heavy-duty double-sided tape (RS components, UK) was
159 used to secure the Teflon bags to the frame. The interior of the plant chamber was
160 only exposed to Teflon surfaces.

161 Compressed air was constantly supplied to the plant chamber via a mass flow
162 controller and regulator (ALICAT MCR-500 SLPM-D, Premier Control Technologies
163 Ltd, UK) at 780 L min^{-1} and 7.5 bar via a 12.7 mm (outer diameter- OD) reinforced
164 tube. This was reduced to approx 1 bar and between 250 to 300 L min^{-1} (+/- 0.8 %)
165 dependent on the photosynthetic and transpiration rate of each plant species
166 (equivalent to one complete air change every 15 - 20 mins). The air stream was
167 passed through a 12.7 mm (OD) PTFE tube to three in-series filters to remove any
168 pre-existing VOCs (activated carbon filter P3KFA14ASMN, Parker Pneumatic, UK),
169 and submicrometer particles (HEPA CAP 75 filter capsule (FDP-780-050K, Fisher
170 Scientific, UK)), and NO_x (Purafil and activated charcoal, Purafil Inc. USA). Finally,
171 the air was re-humidified by passing it through a 2 L Teflon barrel (Jencons, UK)
172 filled with warmed distilled water. The plant chamber outlet air was either vented into
173 the laboratory via a 50 mm (OD) stainless steel pipe and valve, or used to fill an 18
174 m^3 Teflon reaction chamber.

To enhance mixing, air entered the plant chamber via a perforated 12.7 mm (OD) PTFE tube that circled the base of the chamber. One 12.7 mm stainless steel bulkhead fitting (Swagelok, UK) was inserted through the frame to secure the PTFE tube to the base of the plant chamber. A 50 mm (OD) stainless steel pipe was inserted into the upper corner of the chamber and supported by a Teflon (inner surface) and Nylon (outer surface) manifold (Plastics Direct, UK). The manifold also supported an EGM probe (EGM-4, PP Systems, UK), which recorded relative humidity (RH), temperature (T), CO_2 and photosynthetically active radiation (PAR).

Plants were kept in 255 – 330 mm (height) pots depending on species, watered to pot dripping point and sprayed twice weekly. Plant chamber conditions were maintained at 31 – 33.5 °C / 22 – 24 °C (day/night), 29 – 40 % / 33 – 44 % (day/night) RH, and 335 – 385 ppmV / 390 – 404 ppmV (day/night) CO_2. Owing to structural restrictions, PAR could not be measured directly under the growth lamps in the centre of the canopy. At the top edge of the canopy it was 500 μmol m^{-2} s^{-1} with a 12 hr day / night cycle.

2.3 Reaction chamber description

The aerosol photochemical reaction chamber at the University of Manchester is composed of an 18 m^3 FEP Teflon bag mounted on three rectangular extruded aluminium frames (Alfarra et al., 2012). A bank of halogen lamps and a 6 kW Xenon arc lamp are mounted on the enclosure housing the bag, which is coated with reflective "space blanket" providing an integrating sphere, maximising the irradiance

196 in the bag and ensuring even illumination for the production of photochemical species
197 such as the hydroxyl radical (OH). The air introduced to the bag is dried and filtered
198 for gaseous impurities and particles, prior to humidification with high purity
199 deionised water. A high capacity O_3 generator provides controlled ambient levels of
200 O_3 (used as an oxidant) and high O_3 concentrations (serving as a cleaning agent
201 between experiments).

202 Size-dependent (diffusional and gravitational) wall-loss rate constants were calculated
203 based on particle mobility and the surface-to-volume ratio of the chamber (Verheggen
204 and Mozurkewich, 2006). The diffusional loss rate uses a constant of proportionality,
205 which can only be determined empirically. A time period was selected near the end of
206 each experiment where the wall losses were deemed to be the dominant process
207 affecting the size distribution. The volume size distribution at the beginning of this
208 period had the calculated wall loss rate applied to simulate the evolution of the size
209 distribution over the selected time period. If the calculated loss rate loss rate didn't
210 reproduce the measured volume evolution within the specified tolerance (1 – 2 % in
211 this work), the constant of proportionality for diffusional losses was adjusted such that
212 the simulated volume at the end of the selected period matched the measured volume
213 within the specified tolerance. The time-integrated gravitational and (optimised)
214 diffusional loss rate constants were then applied to the volume size distribution
215 throughout the experiment in order to reconstruct a wall loss corrected size
216 distribution, which was then used to calculate the wall-loss-corrected particle mass.

Both the plant chamber and reaction chamber were tested for contaminants separately and when joined together by running the system with an empty plant chamber and by carrying out a "blank" run prior to each set of experiments.

2.4 Analytical techniques

2.4.1 Gas phase measurements

The volatile and semi-volatile organic compounds and oxygenated volatile organic compounds in both the plant chamber and the reaction chamber were measured by soft-ionisation mass spectrometry (PTR-MS, CIR-TOF-MS, described below) and gas chromatography-mass spectrometry (GC-MS).

The proton-transfer-reaction mass spectrometry (PTR-MS) instrument employed (Ionicon, Austria) comprises two turbomolecular pumps, a heated silica steel inlet system and a 9.6 cm long stainless steel drift tube. The nominal response time is approximately 1 s. The operating parameters of the PTR-MS were held constant during measurements, except for the secondary electron multiplier voltage, which was optimised each day. The drift tube pressure, temperature and voltage were 2.2 hPa, 50 °C, and 600 V, respectively. The central reaction chamber of the drift cell was operated at an *E/N* (*i.e.* electric field/gas number density) of 125 Td. The count rate of $H_3O^+.H_2O$ ions was 1 – 2 % of the count rate of H_3O^+ ions. The PTR-MS sampled continuously with a flow rate of 100 – 150 ml min^{-1} through 3.2 mm PTFE tubing.

The chemical-ionisation-reaction time-of-flight mass spectrometer (CIR-TOF-MS) comprises a temperature controlled (40 (±1) ^{o}C) ion-source drift cell assembly coupled to an orthogonal time-of-flight mass spectrometer equipped with a reflectron array (Kore Technology Ltd, Ely, UK). The ion-source deployed was a hollow cathode discharge type (Blake et al., 2009) and the chemical ionization technique used was proton transfer reaction from hydrated hydronium ($H_3O^+.H_2O$) (Jenkin et al., 2012). Sample air was delivered in a continuous stream directly to the drift cell via a 0.5 m long, 6.35 mm (internal diameter) Teflon sample line, heated to 40 (±1) ^{o}C, at a constant flow rate of 80 ml min^{-1}. The central reaction chamber of the drift cell was operated at an *E/N* ratio of ~ 90 – 100 Td, with a tuned energy ramp at the base of the cell to remove potential water-cluster ions (e.g. $RH^+.H_2O$). Further information regarding the CIR-TOF-MS design and a detailed discussion regarding its operation can be found in Blake et al. (2004) and Wyche et al. (2007).

The PTR-MS and CIR-TOF-MS were calibrated using three different methods: (i) step-wise dilution of a gravimetrically prepared gas standard (BOC Special Gases, UK) containing a variety of VOCs and OVOCs; (ii) using calibration material produced in-house via the injection of liquid samples into 10 l Tedlar bags (SKC Inc., USA) containing either humidified or dry, pure nitrogen; and (iii) using gas standards derived from permeation tubes (Vici Inc., US; Ecoscientific, UK), diluted, humidified and delivered by a commercial calibration unit (Kintec, model: 491). Where experimental calibration was not possible for a specific compound, either the calibration sensitivity for a structurally similar surrogate was used or calculated

concentrations were employed (Jenkin et al., 2012). For the quantification of isobaric signals, a single sensitivity value was used, e.g. α-pinene sensitivity for Σ(monoterpenes) and β-caryophyllene sensitivity for Σ(sesquiterpenes); again working on the principal that structurally similar compounds possess similar PTR and CIR sensitivities.

CIR-TOF-MS and PTR-MS detection limits are reagent, reaction, analyte and sample matrix specific. However, typical CIR-TOF-MS detection limits, using PTR ionisation from hydronium, are of the order 0.4 ppbV $(10\ min)^{-1}$ for more polar compounds, such as OVOCs (e.g. 2-hexanone) and as much as 10 ppbV min^{-1} for certain less polar compounds, such as smaller hydrocarbons (e.g. 1-pentene). For further details see Wyche et al., 2007.

The GC-MS system (GC-MS Turbomass Gold, Perkin Elmer, USA) comprised a thermal desorption autosampler (Perkin-Elmer ATD 400) connected via a heated (200 °C) transfer line to a Hewlett-Packard 5890 GC with a 5970 mass-selective detector. Compounds were desorbed at 280 °C for 5 min at 25 mL min^{-1} onto a Tenax-TA cold trap maintained at - 30 °C. The cold trap was then heated to 300 °C for 6 min to desorb compounds onto the GC column. Chromatographic separation was achieved using an Ultra-2 column (Agilent Technologies: 50 m × 0.2 mm ID × 0.11 μm film, 5 % phenylmethyl silica). An initial oven temperature of 35 °C was maintained for 2 min, and then increased at 4 °C min^{-1} to 160 °C followed by an increase of 45 °C min^{-1} to 300 °C, which was maintained for 10 min. The carrier gas was Helium

279 supplied at a rate of 1 mL min^{-1}, with an injector temperature of 250 °C. The limit of
280 detection for isoprene and monoterpenes was approximately 0.25 ng on column and 2
281 ng on column for sesquiterpenes, corresponding to 100 pptV of isoprene, 50 pptV of
282 monoterpenes, and to 400 pptV of sesquiterpenes in a 1 L sample. Sampling was
283 conducted by drawing 8 L of the analyte air through 6.35 mm PTFE tubing onto the
284 GC-MS sample tubes using a handheld pocket pump (SKC Ltd, UK) at a flow rate of
285 150 ml min^{-1} (total sample time ~ 43 mins). Sample tubes were stored at 4 °C until
286 analysed. VOC quantification was by comparison with commercially available liquid
287 standards (Aldrich, Fluka and Sigma) diluted in methanol. Isoprene quantification
288 was by comparison with a 700 ppbV in N_2 certified gas standard (BOC, UK).

289 NO and NO_2 mixing ratios were measured using a chemiluminescence gas analyser
290 (Model 42i, Thermo Scientific, MA, USA). Ozone was measured using a UV
291 photometric gas detector (Model 49C, Thermo Scientific, MA, USA).

292 *2.4.2 Particle phase measurements*

293 Within the main reaction chamber, a scanning mobility particle sizer (SMPS) system
294 was used to measure the particle size distribution and total aerosol mass concentration
295 (without sample drying). A particle density of 1.3 g cm^{-3} was assumed for calculating
296 the mass of SOA particles in un-seeded experiments (Alfarra et al., 2006; Bahreini et
297 al., 2005). For seeded experiments, a density of 1.77 g cm^{-3} was used to calculate the
298 ammonium sulphate seed mass and 1.3 g cm^{-3} was assumed for calculating the
299 additional SOA mass. A water-based condensation particle counter (wCPC, TSI

300 3786) was used to count the total particle number concentration between 2.5 nm and
301 approximately 3 μm. Further instrument details can be found in Alfarra et al., 2012,
302 and references therein.

303 Real-time broad chemical characterisation of the SOA was made using a compact
304 Time-of-Flight Aerosol Mass Spectrometer (cToF-AMS, Aerodyne Research Inc.,
305 USA). A detailed description of the instrument, its operation and calibrations can be
306 found elsewhere (Drewnick et al., 2005;Canagaratna et al., 2007). The instrument was
307 operated in the standard configuration, taking both mass spectrum (MS) and particle-
308 time-of-flight (PToF) data and was calibrated for ionisation efficiency using 350 nm
309 monodisperse ammonium nitrate particles. The vapouriser was set at approximately
310 600 ^{o}C and data were collected at a time resolution of 2 min. A collection efficiency
311 value of unity was applied to these data, based on evidence from a previous chamber
312 study (Alfarra et al., 2006).
313 Filter samples for offline analysis were collected (without denuders) in a specially
314 constructed holder, positioned in the chamber vent line. Aerosol samples were
315 collected onto 47 mm quartz fibre filters (Whatman) at a rapid flow rate of 3 m^3 min^{-1}
316 (sample time ca. 6 mins.). After sampling, filters were immediately placed in pre-
317 cleaned glass vials and stored below -20 °C until analysis. The filter collection
318 procedure employed here is much faster than traditional filter collection methods,
319 which should minimise any potential negative and positive artefacts.

320 The filters were extracted into high purity water, filtered, evaporated to dryness and
321 redissolved in 1 ml 50 % MeOH : 50 % H_2O. The water-soluble compounds were
322 analysed using liquid chromatography-ion trap mass spectrometry (LC-MS/MS).
323 Reverse phase LC separation was achieved using an HP 1100 LC system equipped
324 with an Eclipse ODS-C_{18} column with 5 μm particle size (Agilent, 4.6 mm x
325 150 mm). Samples (60 μl) were injected then eluted by gradient elution with solvents
326 A: 0.1% v/v formic acid water (Optima grade, Fisher) and B: methanol (Optima
327 grade, Fisher) and a gradient program of 3 % B at time 0 min to 100 % B at 60
328 minutes with a flow rate of 0.6 ml min^{-1}. Mass spectrometry analysis was performed
329 in negative ionisation mode using an HCT-Plus ion trap mass spectrometer with
330 electrospray ionisation (Bruker Daltonics GmbH). Electrospray ionisation (ESI) was
331 carried out at 350 °C with a nebuliser pressure of 4.82 bar and a nitrogen drying gas
332 flow of 12 l min^{-1}. Further details can be found in Hamilton et al., 2013.

333 ***2.5 Experimental protocol***

334 Three plants were placed in the plant chamber a minimum of 48 hours prior to the
335 start of the experiment. Both the pots and soil were isolated by enclosing them in
336 PFTE sheeting; this acted to prevent VOC emissions from the plastic pots and soil
337 NO_x emissions from entering the chamber air. Three experiments were carried out on
338 each species over a one-week period, after which the plants were removed and
339 replaced with three plants of the next species, and the experiment cycle repeated.

340 Prior to each experiment, ozone was added to the chamber to give a mixing ratio of
341 approximately 2 ppmV and was left overnight. The chamber was then filled and
342 flushed several times using clean air from the facility's main inlet system (including
343 Purafil, charcoal and HEPA filters as described above), until the total particle count
344 (as measured by a water based condensation particle counter) was below 10 cm^{-3} and
345 the O_3 and NO_x levels were less than 1 and 2 ppbV, respectively. At this point, the
346 reaction chamber was flushed and then connected to the plant chamber for filling with
347 the plant VOC emissions. Aerosol and gas phase composition and concentrations
348 were continuously monitored throughout. At the end of the filling process, the plant
349 chamber was disconnected from the reaction chamber, and within the space of
350 roughly one minute, both the chamber lights were turned on and pure O_3 was injected
351 to provide an initial concentration of around 20 or 70 ppbV (experiment dependent).
352 The switching on of the chamber lights marked the start of each experiment, which
353 typically lasted 6 hours from this point. For experiments using pre-existing seed,
354 polydisperse ammonium sulphate particles (diameter between 40 – 60 nm) were
355 generated from an aqueous solution using an aerosol nebuliser (Topas, ATM 230) and
356 injected without drying into the reaction chamber at the end of the filling from the
357 plant chamber.

358 In our experiments we chose to use ammonium sulphate for the aerosol seeds, rather
359 than acidic particles that could otherwise promote isoprenoid particulate mass
360 formation. Whilst it is recognised that isoprenoid SOA mass can be enhanced by the
361 presence of acidic aerosol seed as originally reported by Jang et al. (2002) and

362 subsequently by Limbeck et al. (2003), Edney et al. (2005), Kleindienst et al. (2007),
363 Limbeck et al. (2007) and Surratt et al. (2007), we have limited our study to SOA
364 formation in the mixed precursor systems without deliberate enhancement of particle
365 mass by condensed phase reaction. There is clear evidence that isoprene oxidation can
366 contribute to atmospheric SOA formation (e.g. Claeys et al., 2004, Edney et al., 2005)
367 and we have previously found that enhancement in SOA from isoprene oxidation
368 above the Bornean rainforest compared with the Amazon may result from an
369 enhanced marine acidic sulphate contribution to sub-micron aerosol (Robinson et al.,
370 2011). Intermediates in SOA formation from isoprene have been identified (e.g. Lin
371 et al., 2012, 2013) and mechanisms for the acid catalysed formation proposed (Surratt
372 et al., 2010). Whilst out of the scope of the current study, this should be the focus of
373 future work.

374 Air samples were taken from three separate locations: 1) immediately before the plant
375 chamber (pre-PC) for blank subtraction, 2) immediately after the plant chamber (post-
376 PC) during the reaction chamber filling period for directly emitted BVOC and 3) from
377 the reaction chamber (RC) during the experiment. RC air was monitored continuously
378 using PTR-MS and CIR-TOF-MS for VOC decay and formation of reaction products.
379 Air samples from the pre-PC and post-PC position, as well as RC air samples
380 immediately at the start of each experiment and 1, 2, 4 and 6 hours after the lights
381 were switched on, were collected on Tenax TA and Carbotrap filled stainless steel
382 tubes (Supelco Inc, PA, USA) for GC-MS analysis.

383 Relative humidity (%), CO_2 (ppmV), PAR (μmol m^{-2} s^{-1}), and temperature (°C) in the
384 plant chamber were recorded every 5 or 10 mins during reaction chamber filling, and
385 every 15 or 20 mins overnight. System blanks were taken at the start and end of the
386 experimental period. The reaction chamber background was checked and
387 characterised through the performance of regular blank experiments (one in every five
388 experiments). NO_x (NO, NO_2 and NO_3) and O_3 were continuously monitored in the
389 reaction chamber. A list of all experiments and their general parameters is given in
390 Table 1.

391 ***2.6 Calculated OH concentrations***

392 Since isoprene losses are controlled by reaction with ozone and the hydroxyl radical
393 (OH), the concentration of OH available to react with isoprene in the reaction
394 chamber for each experiment was calculated based on the measured concentrations of
395 O_3 and isoprene in each experiment, the rate of change in isoprene concentration, and
396 the rate constants for the reactions of isoprene with OH and O_3, using equation (1):

397 $$\frac{\frac{d[Isoprene]}{dt} + k_{O_3}[O_3][Isoprene]}{-k_{OH}[Isoprene]} = [OH] \qquad \text{Eq}^{n}\ (1)$$

398 Hourly averaged concentrations of O_3 and isoprene were calculated for five of the
399 experiments using the tropical fig. Using these data along with equation (1) a range of
400 OH concentrations were obtained. For the first hour after lights on, [OH] was
401 estimated to be $1.9 \times 10^5 - 9.5 \times 10^5$ molecules cm^{-3}, whereas, towards the end of the

experiment after roughly five hours, values of 8.1 x 10^5 – 1.9 x 10^6 molecules cm^{-3} were obtained. In general, during the tropical fig experiments, [OH] estimated from isoprene and ozone was observed to steadily increase over the duration of the experiment from 0 – 5 hours after lights on.

2.7 VOC/NO_x Conditions

Figure 1 shows the time-dependent mixing ratios of ozone and oxides of nitrogen for each experiment set. Although every effort was made to keep the concentrations of oxides of nitrogen low, measurable amounts were present, giving initial VOC/NO_x ratios of the order 2 – 6 and 3 – 9 (see Table 1), for the birch and fig experiments, respectively (where here, the VOC concentration is equal to the sum of all potential precursor concentrations). In terms of a "Sillman plot" (Sillman, 1999), the experiments were carried out in the "VOC sensitive regime".

The absolute concentration of VOCs in the reaction chamber was roughly ten times greater than those measured over the rainforest during our field experiments (Mackenzie et al., 2011) and the VOC/NO_x ratios employed here were as much as ten times lower (i.e. typical ratio of 20:1, isoprene:NO_x over the rainforest) (Hewitt et al., 2010b). The source of the NO_x in the reaction chamber (initially ~ 2 – 6 ppbV NO_x, but increasing to ~ 5 – 9 ppbV after ~ 5 hours) is attributed to a small amount of diffusion of outside ambient air across the porous Teflon membrane into the reaction chamber. The production of certain reactive intermediates in the oxidation of VOCs

422 (e.g., hydroxyl hydroperoxides from isoprene oxidation) is very sensitive to NO_x
423 concentrations in the reaction mixture.

424 **Results**

425 ***3.1 Experiments with Betula pendula***

426 *3.1.1 Gas phase*

427 Continuous gas phase monitoring with the CIR-TOF-MS and PTR-MS throughout the
428 experiments, indicated successful transfer of VOC precursor material from the plant
429 chamber to the reaction chamber prior to lights on. The data indicated that there was
430 negligible loss of precursor compounds during the chamber transfer process (Fig. 2a).

431 Immediately after initiation of the photochemistry, the VOC precursor concentrations
432 were observed to decay and product ions began to appear in the CIR and PTR mass
433 spectra. Approximately sixty product-ion peaks were observed by the CIR-TOF-MS
434 and the PTR-MS in the organic gas phase during a typical *Betula pendula* experiment.
435 The temporal profiles of a number of the most abundant (O)VOCs measured are
436 shown in Fig. 2. From a combination of the CIR-TOF-MS, PTR-MS and GC-MS
437 observations (and from those observations discussed below for the tropical plant
438 experiments), over fifty different hemi-, mono- and sesqui-terpene oxidation products
439 were tentatively identified (Fig. 3 and Tables S1 – S5 in the supplementary
440 information).

441 From initial inspection of the data, it is clear that monoterpenes dominate during the
442 *Betula pendula* experiments (Fig. 2a and b), with strong signals observed in the CIR-
443 TOF-MS and PTR-MS mass spectra at *m/z* 137 (protonated parent ion) and 81
444 (hydrocarbon fragment). A small amount of isoprene was also detected during *Betula*
445 *pendula* experiments; however this was always significantly lower in magnitude than
446 that of the sum of monoterpenes; for example, during the experiment on 07/07/09,
447 12.6 (± 3.8) ppbV monoterpenes were measured in the reaction chamber prior to
448 lights on (c.f. 11.4 ppbV total monoterpenes measured at the post-PC position by the
449 GC-MS), whereas only 2.0 (± 1.0) ppbV isoprene was detected. Speciation of the
450 monoterpenes by GC-MS indicated that the most dominantly emitted C_{10} compounds
451 from *Betula pendula* were α- and β-pinene (Table 2).

452 C_{15} sesquiterpenes (parent ion *m/z* 205) were detected in the plant and reaction
453 chambers during each *Betula pendula* experiment, with the most abundant species
454 identified by GC-MS being β-caryophyllene (Table 2). Sesquiterpenes were also
455 measured in the reaction chamber by CIR-TOF-MS (Fig. 2c), however for the
456 majority of the experiments they were present at concentrations either close to or
457 below the detection limit, hence they could not always be monitored as a function of
458 reaction time. For the experiment on 07/07/09, 1.7 (± 0.9) ppbV sesquiterpenes were
459 measured by the CIR-TOF-MS prior to lights on (c.f. 2.2 ppbV total sesquiterpenes
460 measured at the post-PC position by the GC-MS). An ion of *m/z* 153 was also
461 observed in the PTR and CIR mass spectra of the plant chamber emissions and

462 subsequently in the reaction chamber air, tentatively assigned (and here after referred
463 to) as camphore.

464 During the reaction phase of the *Betula pendula* experiments the CIR-TOF-MS mass
465 spectra were dominated by ions of relatively high mass (i.e. $m/z > 100$) pertaining to
466 products of both monoterpene and sesquiterpene oxidation. The ions of highest mass
467 (i.e. m/z 170 – 290) are characteristic of sesquiterpene oxidation, and have been
468 observed recently during a similar chamber study investigating β-caryophyllene
469 photo-oxidation (Jenkin et al., 2012). Drawing a comparison between these data and
470 the detailed β-caryophyllene study conducted by Jenkin et al. (2012), a number of
471 tentative assignments have been made for β-caryophyllene products, with the
472 assumption that other precursor specific structural isomers may also occupy the same
473 mass channels. A full list of example tentative assignments is given in the
474 supplementary information (Table S2). In total the sum of all sesquiterpene products
475 measured in the chamber was estimated to be ~ 1.5 ppbV (assuming an average PTR
476 sensitivity for such high mass, oxygenated, compounds).

477 In contrast to the small amounts of sesquiterpene products observed in the reaction
478 chamber, the products observed in greatest abundance were those derived from
479 monoterpene decay. The largest (combined) product signal measured by the CIR-
480 TOF-MS was that of $\Sigma(I_{111}, I_{93})$, where I_x is the intensity of the mass spectrum at m/z
481 = x (Fig. 2d). Previously, the m/z 111 and 93 signals have been shown to correspond
482 to various primary C_7 unsaturated aldehydes formed during the oxidation of

483 unsaturated acyclic monoterpenes, such as myrcene, ocimene and linalool (Lee et al.,
484 2006a; Lee et al., 2006b; Ng et al., 2006; Wyche et al., In Preparation). In the case of
485 myrcene and ocimene, the *m/z* 111 and 93 signals correspond to the parent ion (MH^+)
486 and the dehydrated daughter fragment, respectively (MH^+-H_2O), and in the case of
487 linalool *m/z* 111 corresponds to the dehydrated daughter ion and *m/z* 93 is a further
488 fragment. The concomitant *m/z* 111 and 93 signals have also been reported to result
489 from a C_7 cyclic ketone formed during the oxidation of terpinolene (not found in the
490 *Ficus* emission profile and < 1 ppbV found in the *Betula* profile). The *m/z* 111 and 93
491 ions have previously been observed to be significant contributors to total ion signal in
492 the PTR mass spectra during single precursor chamber experiments with concomitant
493 SOA formation (Lee et al., 2006a; Lee et al., 2006b; Ng et al., 2006; Wyche et al., In
494 Preparation), and the *m/z* 111 ion has also been observed in ambient air measurements
495 over a forested region (Holtzinger et al., 2005).

496 As can be seen from observation of Fig. 2(d), the $\Sigma(I_{111}, I_{93})$ signal rises rapidly
497 during the initial stages of the experiment, much more so than other monoterpene
498 oxidation products (c.f. Fig. 2e), suggesting that the precursor has a much shorter
499 lifetime with respect to OH and O_3. Of those monoterpenes speciated by the GC-MS,
500 ocimene and linalool have the shortest lifetimes, with k_{OH} = 3.04 and 1.6×10^{-10} cm^3
501 $molecule^{-1}$ s^{-1} (average lifetimes with respect to OH ~ 44 and 55 mins.), respectively,
502 compared to $k_{OH} = 7.4 \times 10^{-11}$ cm^3 $molecule^{-1}$ s^{-1} for β-pinene (average lifetime with
503 respect to OH ~ 1458 mins.) (Atkinson and Arey, 2003; Kim et al., 2011). The $\Sigma(I_{111},$

504 I_{93}) signal peaks at around 60 – 100 mins at 3.0 (± 0.7) ppbV (concentration estimated
505 using pinonaldehyde sensitivity), before decaying at a greater rate than that of the
506 precursor monoterpenes and the other monoterpene products. This relatively short
507 lifetime gives further insight into the potential identity of the *m/z* 111 and 93 signals,
508 perhaps indicating the presence of multiple C=C bonds in the hydrocarbon structure,
509 as would be found in the primary C_7 aldehydes obtained from the oxidation of
510 ocimene or myrcene for example. Other short-lived biogenic oxidation products that
511 could exist in such mesocosm systems, include α-hydroxy carbonyls, similarly formed
512 following OH addition to a C=C bond.

513 Other dominant signals observed by the PTR-MS and CIR-TOF-MS during oxidation
514 of the *Betula pendula* air matrix, include the sum of *m/z* 169 + 151 + 107, which
515 respectively correspond to the parent ion and two daughter fragments of a number of
516 primary monoterpene keto-aldehydes (which, from the speciated monoterpene plant
517 chamber data, are most likely to be pinonaldehyde, caronaldehyde and α/γ-
518 terpinaldehyde); and *m/z* 139, corresponding to the parent ion of a number of primary
519 monoterpene ketones (most likely to be nopinone and caronone, again when
520 considering the monoterpenes speciated by the GC-MS). As shown in Fig. 2(e) the
521 primary keto-aldehyde and ketone signals had similar temporal profiles to one
522 another, growing at a slower rate than that of $\Sigma(I_{111}, I_{93})$, to peak concentrations of
523 around 0.9 (± 0.3) and 1.2 (± 0.3) ppbV, respectively, as the monoterpene trace
524 tended towards zero. The temporal profile for the sum of all other "monoterpene
525 like" product ions (i.e. ions of *m/z* > 90) was very similar to those of the primary keto-

526 aldehyde(s) and ketone(s), peaking at a combined mixing ratio of approximately 3.5
527 ppbV (assuming an average PTR sensitivity for such high mass, oxygenated,
528 compounds).

529 During the oxidation of compounds emitted by *Betula pendula*, the primary isoprene
530 products, methyl vinyl ketone (MVK) and methacrolein (MACR) (measured together
531 at *m/z* 71) were observed to evolve in the same manner as the primary monoterpene
532 keto-aldehyde(s) and ketone(s), peaking at an approximate mixing ratio of 0.4 (± 0.1)
533 ppbV (Fig. 2e). A series of lower *m/z* ions were also observed to evolve within the
534 reaction chamber, including *m/z* 61 (acetic acid), 59 (acetone), 47 (formic acid), 45
535 (acetaldehyde), 33 (methanol) and 31 (formaldehyde). Each of these compounds has
536 previously been associated with monoterpene oxidation and/or with off-gassing from
537 illuminated chamber walls. Methanol, acetone and *m/z* 99 (potentially cis-3-hexenal)
538 were also observed within the reaction chamber prior to lights on, with a combined
539 mixing ratio of approximately 20 ppbV.

540 *3.1.2 Particle phase*

541 From inspection of the CPC and SMPS data we see that SOA mass formed during
542 oxidation of the *Betula pendula* air matrix. As can be seen from Fig. 4, during
543 unseeded experiments nucleation occurred immediately after lights on, with no
544 induction period prior to mass formation. After nucleation, SOA mass increased
545 rapidly to ~11 μg m^{-3} by ~40 minutes (experiment 06/07/09), followed by a relatively
546 stable plateau (after the application of wall loss corrections) and a slight increase

547 towards the end of the experiment. In order to suppress nucleation, seed particles were
548 introduced in some experiments, as has been used previously (Dommen et al.,
549 2009;Meyer et al., 2009;Surratt et al., 2007;Kleindienst et al., 2006;Carlton et al.,
550 2009). This more closely represents the conditions encountered in the ambient
551 atmosphere where there is pre-existing aerosol. Consistent with the nucleation
552 experiments described above, SOA mass was observed to increase as soon as the
553 photochemistry was initiated when an ammonium sulphate seed was present (Fig. 4,
554 experiment 07/07/09).

555 Using the wall-loss-corrected mass data, along with the corresponding quantity of the
556 sum of precursor species reacted and equation (2), SOA yields were obtained for the
557 *Betula pendula* oxidation system:

558 $$Y_{SOA} = \frac{M_P}{\Delta(\Sigma VOC)} \qquad \text{Eq}^{n}\,(2)$$

559 In this instance, Y_{SOA} = SOA mass yield, M_P = peak SOA mass (μg m^{-3}) and $\Delta(\Sigma VOC)$
560 = the sum of gas phase precursors reacted by the time M_p is reached (μg m^{-3}) (Odum
561 et al., 1997). In order to determine $\Delta(\Sigma VOC)$, the time-dependent VOC mixing ratios
562 for total sesquiterpenes, total monoterpenes, camphore and isoprene were
563 independently converted to their corresponding mass concentrations (μg m^{-3}) and the
564 four data sets were combined to give a "total" VOC precursor decay profile. From
565 the total VOC profile, $\Delta(\Sigma VOC)$ was calculated, using the starting mass of ΣVOC at
566 time = 0 and the mass of ΣVOC at the time of M_p. The uncertainty in $\Delta(\Sigma VOC)$ is

567 estimated to be ± 41 %. Using equation (2) for the two *Betula pendula* experiments
568 for which both gas phase mixing ratio and wall-loss-corrected aerosol data were
569 available, SOA yield values of 39 and 26 % were obtained (Fig. 4). It should also be
570 noted that along with previous caveats made regarding the role of the chamber walls
571 and other measurement uncertainties, these yield values also do not take into account
572 the potential loss of particularly "sticky" low volatility compounds (e.g. Ehn et al.,
573 2014) to internal surfaces of the chamber.

574 It should be noted in the above yield calculations that the partitioning of material
575 between the vapour phase and chamber walls has not been taken into account.
576 Matsunaga and Ziemann (2010) showed that semi-volatile organic compounds move
577 towards equilibrium between the walls and the vapour phase and that the equilibration
578 timescale and equivalent absorptive mass of the walls was dependent on the
579 molecular properties of the partitioning species. Kokkola et al. (2013) demonstrated in
580 their model study that OVOC wall losses will have significant implications on their
581 partitioning between the gas and particle phase, such that the mass components of
582 very low volatility will almost completely be depleted to the chamber walls during the
583 experiment while the depletion of OVOCs of higher volatilities is less efficient. The
584 implications of such partitioning to chamber walls are such that comparison between
585 any yields determined experimentally in different chambers should be conducted with
586 caution. Even when calculated from experiments in the same chamber, yields should
587 be interpreted qualitatively and relatively and not extrapolated to the atmosphere.

588 ***3.2 Experiments with tropical species***

589 *3.2.1 Gas phase*

590 In order to study the contrast between species that primarily emit monoterpenes and
591 those that primarily emit isoprene, and hence to better understand the isoprene-SOA
592 system, the coupled plant chamber-reaction chamber system was employed to study
593 several tropical species. Two species of fig and one species of palm were selected
594 during the pre-experiment screening process. Those experiments using the figs, *Ficus*
595 *cyathistipula* and *Ficus benjamina* gave the most complete data set; hence their
596 results are used as a focus for discussion.

597 Fig. 5 shows the temporal evolution of a number isoprenoids detected in both the
598 plant and reaction chambers (a and b) and the concomitant evolution of a selection of
599 isoprenoid oxidation products (c and d), during a typical *Ficus benjamina* experiment
600 (23/06/09). During a typical *Ficus benjamina* experiment, approximately thirty
601 precursor and product-ion peaks were observed by the CIR-TOF-MS and PTR-MS in
602 the gas phase. Tentative product identification is reported in the supplementary
603 information (Fig. 6, Tables S1 – S5). A similar set of ions was observed during a
604 typical *Ficus cyathistipula* experiment.

605 From inspection of Fig. 5(a) and (b), the dominance of isoprene in the *Ficus*
606 *benjamina* system is clear, with 12.3 (± 4.1) ppbV isoprene detected in the reaction
607 chamber at lights on, compared to 0.8 (± 0.4) ppbV monoterpenes, 0.5 (± 0.9) ppbV

608 sesquiterpenes and an estimated 2.7 (± 0.6) ppbV camphore. Speciation of the
609 monoterpenes by GC-MS indicated that the most dominantly emitted C_{10} compounds
610 for *Ficus benjamina* were α-pinene, limonene, sabinene and linalool and for *Ficus*
611 *cyathistipula* were α-pinene, β-pinene and limonene (Table 2). The sequiterpenes, β-
612 caryophyllene and α-cubebene were also identified.

613 Products of isoprene were observed to dominate the evolving *Ficus benjamina* and
614 *Ficus cyathistipula* oxidation systems, with the isobaric primary species MACR and
615 MVK comprising the strongest signals (measured together at *m/z* 71). For example,
616 during the *Ficus benjamina* experiment of 23/06/09, a combined peak MACR + MVK
617 mixing ratio of 2.9 (± 0.7) ppbV was observed (Fig. 5c).

618 Along with MACR and MVK, a series of other ions also associated with isoprene
619 oxidation were detected during *Ficus benjamina* oxidation, including *m/z* 117 and 99
620 (4-hydroxy-2-methyl-but-2-enoic acid), 103 (C5-alkenediols, C4-hydroxydialdehydes
621 and MPAN), 87 (C4-hydroxycarbonyls and methacrylic acid), 83 (3-methyl furan), 75
622 (hydroxy acetone) and 31 (formaldehyde). Additionally, a signal of *m/z* 101 was also
623 measured, possibly corresponding to the sum of a series of C5-hydroxycarbonyls and
624 C5-hydroxy hydroperoxides (Tuazon and Atkinson, 1990; Paulson and Seinfeld,
625 1992; Jenkin *et al.*, 1997; Benkelberg *et al.*, 2000; Sprengnether *et al.*, 2002,
626 Benkelberg *et al.*, 2000; Zhao *et al.*, 2004; Surratt *et al.*, 2006;
627 http://mcm.leeds.ac.uk/MCM, v3.1). Of the signals observed, those of *m/z* 83 and 87
628 (tentatively assigned to be 3-methyl furan and C4-hydroxycarbonyls/methacrylic

629 acid), were the greatest in magnitude after MACR + MVK (Fig. 6). The temporal
630 evolution of the sum of all of these products suggests that they are predominantly
631 secondary in nature, forming in the chamber after MACR and MVK. They continued
632 to increase in magnitude as the isoprene signal decreased and as the MACR + MVK
633 signal began to fall (Figs. 5 and 6). During a typical *Ficus benjamina* experiment, the
634 sum of these isoprene products was estimated to reach a peak mixing ratio of ~ 1.7
635 ppbV.

636 A series of lower molecular weight ions were also observed to evolve within the
637 reaction chamber, including *m/z* 61 (acetic acid), 47 (formic acid), 45 (acetaldehyde),
638 33 (methanol) and 31 (formaldehyde). Each of these compounds has previously been
639 associated with isoprene oxidation and/or with off-gassing from illuminated chamber
640 walls. The *m/z* 43 and 46 signals, indicative of carbonyls and nitrates, respectively,
641 were also observed to increase significantly during photo-oxidation, indicating the
642 formation and evolution of such species with increasing experiment duration.

643 Besides ions pertaining to the oxidation products of isoprene, a number of spectral
644 features typically derived from monoterpene oxidation products were also observed to
645 form and evolve in the reaction chamber, including, *m/z* 151, 125, 109, 107, 93 and
646 91. To a first order approximation, the total peak quantity of oxidation products not
647 believed to result from isoprene decay was estimated to be of the order 2 ppbV.
648 However, it should be noted that the presence of isobaric interference in such a
649 complex system, uncharacterised fragmentation, detection limits and the use of

650 pseudo and averaged calibration sensitivities, impose a certain level of unknown
651 uncertainty upon this final value.

652 *3.2.2 Particle phase*

653 Contrary to the immediate and abundant formation of new particles in the un-seeded
654 *Betula pendula* experiments, the total number of particles and total aerosol mass did
655 not increase above background levels after lights were turned on in the un-seeded
656 tropical *Ficus benjamina* experiments. Figure 7 shows the observed and wall-loss-
657 corrected particle mass concentration during two typical *Ficus benjamina* experiments
658 (22/06/09 and 23/06/09) along with a chamber background experiment. Owing to a
659 lack of particle nucleation in those experiments, the total particle number
660 concentration was too low for the wall loss correction (described in section 2.3) to be
661 implemented. Instead, the average of the wall loss constants determined for the
662 seeded experiments was used to calculate the wall loss corrected mass concentrations
663 reported in Figure 7.

664 Figure 8 shows the observed and wall-loss-corrected particle mass concentration for
665 ammonium sulphate seeded experiments using VOC emissions of *Ficus benjamina*
666 and *Ficus cyathistipula*, as well as a seeded background experiment. The mass at the
667 start of the experiment represents the initial ammonium sulphate mass. In order to
668 quantify the formation of SOA mass during these experiments, the mass increase
669 relative to the starting seed mass was determined in Figure 9 by subtracting the initial
670 ammonium sulphate seed mass from the total wall loss corrected mass. The same

calculation was also performed for the *Betula pendula* seeded experiment (07/07/09). In contrast to the unseeded *Ficus benjamina* and *Ficus Cyathistipula* experiments, SOA mass was observed to form when a seed was present in the reaction chamber. The calculated SOA traces in Figure 9 illustrate a slower build-up of mass during the isoprene dominated *Ficus benjamina* (15/07/09) and *Ficus Cyathistipula* (30/06/09 and 02/07/09) experiments compared to the much faster SOA mass formation in the monoterpene dominated *Betula pendula* experiment. Peak masses of the order 1.3 – 5.5 μg m^{-3} were observed, which when employed with the methodology described in section 3.1.2, produce SOA yields of 10 and 14 % for each of the two *Ficus Cyathistipula* experiments for which both gas and wall-loss-corrected aerosol data were available, i.e. 30/06/09 and 02/07/09, respectively (Fig. 9). Uncertainty in $\Delta(\Sigma VOC)$ is estimated to be ± 47 % and in the size distribution measurements used in the wall loss calculations, of the order of ± 2 %. The uncertainties in the wall-loss correction will likely be substantially greater, but remain unquantified at present.

Discussion and Conclusions

4.1 Betula pendula

In this study we coupled a plant chamber to a photochemical reaction chamber in order to investigate secondary organic aerosol production from a biogenically consistent mixture of biogenic volatile organic compounds. We studied silver birch

690 (*Betula pendula*), which emits predominantly monoterpenes, with some
691 sesquiterpenes and oxygenated VOCs but only trace isoprene (Table 2, Fig 3).

692 Our *Betula pendula* experiments showed significant SOA formation (Fig. 4) both in
693 the presence and absence of an ammonium sulphate seed, and reproduced the rate of
694 production and growth of SOA observed in earlier published studies (Mentel et al.,
695 2009;Carlton et al., 2009;e.g. VanReken et al., 2006;Hallquist et al., 2009;Kiendler-
696 Scharr et al., 2009a;Kiendler-Scharr et al., 2009b).

697 The SOA yield values of 39 and 26 % obtained here for *Betula pendula* compare
698 reasonably well with those reported within the literature for single precursor work
699 conducted under similar conditions. For instance, for the two most abundant
700 monoterpenes emitted by *Betula pendula*, i.e. α-pinene and β-pinene, single
701 precursors yields of the order 1 – 43 (16) and 3 – 30 %, respectively, have been
702 observed (values given in parenthesis were obtained from the Manchester aerosol
703 chamber). Similarly for other common monoterpenes such as limonene, myrcene, Δ3-
704 carene and α-terpenine, SOA yields of 9 – 34, 6 – 43 (15), 2 – 38 and 8 – 25 %,
705 respectively, have been reported and for β-caryophyllene, 37 – 79 (50) % (Lee at al.,
706 2006a and references therein; Alfarra at al., 2012). In a comparable study to ours,
707 Mentel et al., (2009) reported a fractional mass yield of 11 % for their *Betula pendula*
708 experiments, i.e. slightly lower than those given here, but within the bounds of
709 quantified experimental errors. The yield values obtained here for the *Betula pendula*
710 mesocosm system lie roughly in the middle of the single precursor yield range.

711

712 As can be seen from inspection of Fig. 3, the transfer of mass through the *Betula*
713 *pendula* experiment appeared roughly conservative, with a small and steady loss of
714 measured mass from the reaction matrix after ~ 220 min. With the addition of
715 oxygen to the starting body of hydrocarbon material during such an experiment, the
716 total measured mass (i.e. ΣVOCs + SOA) within the system would be expected to
717 increase with time. The absence of such a total measured mass gain (and indeed the
718 mass deficit observed towards the end of the experiment), can most likely be
719 accounted for by considering the various measurement uncertainties involved in
720 producing these data (e.g. assumptions in PTR sensitivity, uncharacterised
721 fragmentation following ionisation, instrument detection limits, etc.) and influences
722 imposed by the chamber walls (including potential loss of more highly oxidised
723 material from the gas phase and greater than expected loss of SOA). Indeed, there is
724 potential for a system mass increase by the end of the experiment to lie within the
725 uncertainty bounds of the CIR-TOF-MS/PTR-MS measurements alone, e.g. the
726 average, single compound PTR measurement uncertainty is ~ ± 30 %, allowing the
727 final measured value of 130 μg m^{-3} to have an upper limit of 170 μg m^{-3}, i.e. greater
728 than the starting value. Considering these results it seems that the system studied is
729 reasonably well characterised given the complications involved in such a task.

730 Certain insights into the mechanisms of SOA formation and growth during the *Betula*
731 *pendula* experiments can be obtained through a combined examination of the VOC

732 data, the time-dependent growth curves (Fig. 10) and the aerosol composition data.
733 The data in Fig. 10 demonstrates that during oxidation of the *Betula pendula*
734 emissions and in absence of a seed, SOA mass evolution can be roughly split into two
735 phases. In the early stages of the experiment after nucleation, SOA mass growth
736 increased somewhat rapidly with respect to the amount of precursors reacted;
737 however, after roughly 30 % of the initial precursor mass had been consumed, the rate
738 of mass growth with respect to VOC precursor consumption was observed to reach an
739 approximate steady state. When ammonium sulphate seed was present within the
740 chamber, there was a similarly rapid initial growth with respect to VOC consumption,
741 however this time subsequent aerosol evolution was characterised by a roughly linear
742 mass increase to a much higher final mass by the end of the experiment. Considering
743 the various species of precursor VOCs detected in the *Betula pendula* plant chamber
744 air, and the relative lifetimes of these VOCs, it would seem possible that initially the
745 shorter-lived sesquiterpenes react to form a significant proportion of the high mass,
746 nucleating/condensing species, before being removed from the system (e.g. Jenkin et
747 al., 2012). Subsequent aerosol mass formation as the air in the reaction chamber ages
748 towards the central phase of the experiment, is then likely to result from the
749 partitioning of relatively more volatile products formed from slower reacting
750 monoterpenes, e.g. products such as pinic and pinonic acid from α-pinene oxidation
751 (e.g. Jenkin, 2004; Camredon et al., 2010), and products such as the primary acyclic
752 unsaturated aldehydes, (*m/z* 111 + 93); the temporal profile of which demonstrates

753 gas-phase loss concomitant with wall-loss-corrected aerosol growth reaching a steady
754 state.

755 Further understanding of the composition and evolution of SOA typical of temperate
756 plant environs comes from investigation of Figure 11, which shows the evolution of
757 the fraction of the ratio of more/less oxygenated material present in the aerosol during
758 the initial stages of a typical unseeded *Betula pendula* experiment (06/07/09). Figure
759 11 was constructed using the ratio of *m/z* 44 to 43 obtained from the AMS (*i.e. f*44/43,
760 where *m/z* 44 is derived from "more" oxidised material and *m/z* 43 from "less"
761 oxidised material, Ng et al., 2010). In this instance, the *f*44/43 ratio exhibits linear
762 growth with time, from a value of ~ 0.8 to ~ 1.1, suggesting an increase in the
763 oxygenated content of the aerosol as the experiment ages. Such an increase in
764 oxygenated content is generally observed when precursor species contain multiple
765 C=C bonds (e.g. ocimene and myrcene), offering significant potential for higher
766 aerosol O:C composition (e.g. perhaps species such as acyclic unsaturated aldehydes
767 and their subsequent generations of products). Indeed, the evolution of the *f*44/43
768 ratio observed here is consistent with those results obtained from single precursor
769 experiments investigating the acyclic monoterpene, myrcene and the sesquiterpene, β-
770 caryophyllene (Alfarra et al., 2012; Alfarra et al., 2013).

771 Off-line compositional analysis of the SOA collected at the end of the *Betula pendula*
772 experiments supports the findings obtained from the on-line gas phase and bulk
773 aerosol composition data. The LC-MS^2 analysis produced chromatograms with peaks

774 matching those seen in comparable single precursor BVOC experiments, with tracer
775 compounds of both sesquiterpene and monoterpene SOA, detected (Fig. 12).
776 Amongst the compounds observed were those of molecular weight (MW) 238, 242,
777 254 and 256, corresponding to 4-(3,3-dimethyl-2-(3-oxopropyl)cyclobutyl)pent-4-
778 enoic acid, 3-(3,3-dimethyl-2-(3-oxobutyl)cyclobutyl)-3-hydroxypropanoic acid, β-
779 nocaryophyllonic acid/β-caryophyllinic acid and β-nocaryophyllinic acid,
780 respectively, produced during β-caryophyllene oxidation (e.g. Alfarra et al., 2013)
781 and MW 184, corresponding to cis-pinonic acid, produced during α-pinene oxidation.
782 Many other terpene oxidation tracers were detected, including compounds of
783 molecular weight 118 and 200, which are also prevalent in SOA obtained from single
784 precursor myrcene experiments. This observation is in line with findings obtained
785 from the gas phase data, which suggest a relatively significant presence of gaseous
786 acyclic unsaturated aldehydes that would originate from acyclic unsaturated terpenes,
787 such as myrcene.

788 ***4.2 Tropical species***

789 In addition to *Betula pendula*, we studied three tropical plant species: two figs (*Ficus*
790 *benjamina* and *Ficus cyathistipula*) and one palm (*Caryota millis*); in this work, we
791 focus on results obtained from the fig plants. All three tropical species were found to
792 be strong isoprene emitters, with very much smaller emissions of monoterpenes,
793 sesquiterpenes, and oxygenated VOCs (Table 2, Fig. 6).

794 During the tropical plant experiments, the primary gas-phase isoprene oxidation
795 products MACR, MVK, formaldehyde, isoprene hydroxy hydroperoxides and the
796 secondary product hydroxyacetone were all observed (e.g. Figs. 5 and 6 and Tables
797 S4 and S5 in the supplementary information). MACR, the isoprene hydroxy
798 hydroperoxides (isoprene epoxide (IEPOX) and isoprene hydroperoxide (ISOPOOH))
799 and hydroxyacetone are all believed to be precursors to SOA formation (Jaoui et al.,
800 2010;Carlton et al., 2009;Kleindienst et al., 2009;Paulot et al., 2009;Kleindienst et al.,
801 2007;Lee et al., 2006;Kroll et al., 2006;Surratt et al., 2006;Claeys et al.,
802 2004b;Rollins et al., 2009;Robinson et al., 2010). In this study, with the exception of
803 MACR and MVK, these products all formed at yields lower than those previously
804 reported (Table 3), with MACR + MVK, hydroperoxides, hydroxy acetone and
805 formaldehyde being observed to form in yields of 17 – 36, 1 – 3, 0 – 2 and 2 – 7 %,
806 respectively during our work. This disagreement may result from differences in OH
807 concentrations and NO_x concentrations in each of the experimental studies. Other
808 isoprene products tentatively identified from the CIR-TOF-MS and PTR-MS data
809 include, C5-alkenediols, C4-hydroxycarbonyls/methacrylic acid and 3-methyl furan
810 (Table S4), which have also previously been associated with SOA formation (e.g.
811 Claeys et al., 2004; Surratt et al., 2006; Robinson et al., 2010). For a typical *Ficus*
812 *benjamina* experiment (23/06/09) the sum of these and other potential isoprene
813 products, excluding MACR + MVK, was estimated to have a combined gas phase
814 yield of the order 18 % (Fig. 5).

As can be seen in Fig. 6 mass transfer through the *Ficus benjamina* system was characterised by a slight mass decrease just after the start of the experiment followed by a gradual increase in mass with time. As was stated in section 4.1 a mass increase is expected with time during such an experiment, owing to the addition of oxygen to the precursor hydrocarbon material. Consequently, when considering the data presented in Fig. 6 in the context of potential uncertainties involved (including difficult to characterise influences imposed by the chamber walls), it appears that the system being studied is reasonably well characterised.

By comparing Figs. 3 and 6 we see that the monoterpene dominated *Betula pendula* system, which produces larger and lower vapour pressure oxidation products than the isoprene dominated *Ficus* system, as well as measureable SOA, is the case which exhibits measured mass loss. From this contrast it is reasonable to assume a significant fraction of any mass deficit observed during *Betula pendula* oxidation could result from the loss of the heavier, lower volatility compounds that are present in the *Betula pendula* oxidation system but not in the *Ficus* system.

Despite the detection of a number of first- and second-generation gas phase products that have previously been directly linked with isoprene SOA composition (Claeys et al., 2004; Wang et al., 2004; Edney et al., 2005; Surratt et al., 2006; Healy et al., 2008), there was no accompanying evidence of SOA formation from the isoprene-emitting tropical plants during unseeded, nucleation style experiments (Fig. 7). A lack of SOA mass formation during our unseeded *Ficus benjamina* experiments could have resulted from a number of different factors, not least of which was simply the

837 absence of a seed surface (acidic or otherwise) to help facilitate partitioning of the
838 semi-volatile oxidation products to the aerosol phase and produce particles of
839 sufficient size and measureable particle mass (e.g. Kroll et al., 2006). Another
840 potentially significant contributing factor in suppressing SOA formation during these
841 experiments was our relatively low VOC/NO_x ratio and the resultant gas phase
842 chemistry. In the presence of high (i.e. ppbV-level) NO_x mixing ratios, RO_2 radicals
843 react with NO to produce mainly alkoxy (RO) radicals. For low molecular mass
844 VOCs such as isoprene, these RO radicals generally fragment into smaller, more
845 volatile products that do not easily partition from the gas phase to the aerosol phase,
846 resulting in a low SOA yield (Surratt *et al.,* 2010). Conversely, under low NO_x
847 conditions, RO_2 radicals are known to undergo self- and cross-reactions to produce
848 organic peroxides and hydroperoxides of relatively low volatility. For example,
849 Surratt *et al.* (2010) showed that under high NO_x conditions the yield of the
850 potentially SOA forming gas phase IEPOX was reduced with respect to the equivalent
851 value under low NO_x conditions, where IEPOX formed in substantial yields (upward
852 of 75 %) from the further oxidation of ISOPOOH by OH.

853 In contrast to our unseeded *Ficus* experiments, when an ammonium sulphate seed was
854 present (and following wall loss correction), SOA mass was observed to form and
855 evolve within the reaction chamber (Fig. 9). From estimates of the total
856 concentrations of precursor VOCs within the reaction chamber matrix (primarily
857 isoprene, e.g. Fig. 5), an SOA mass yield of the order 10 – 14 % was obtained for the
858 *Ficus Cyathistpula* system. If it were to be assumed that the SOA were solely formed

859 from oxidation products of isoprene as the major emitted VOC, this yield would
860 appear excessive in comparison with those obtained previously from single precursor
861 isoprene studies, i.e. ~ 0.1 – 5.5 % (van Donkelaar et al., 2007;Kleindienst et al.,
862 2009, 2007;Kroll et al., 2005, 2006;Claeys et al., 2004a;Edney et al., 2005(van
863 Donkelaar et al., 2007;Kleindienst et al., 2009, 2007;Kroll et al., 2005, 2006;Claeys et
864 al., 2004a;Edney et al., 2005; Brégonzio-Rozier et al., 2014). However, we must
865 consider that the mesocosm system is in fact an ensemble of precursors, albeit an
866 ensemble dominated by isoprene, analogous to ambient air above a tropical forested
867 region (Hewitt et al., 2010; MacKenzie et al., 2011).

868 For the experiments of 30/06/09 and 02/07/09, for which SOA yields were obtained
869 for the *Ficus Cyathistpula* system, a fraction of camphore was also observed in the air
870 entering the reaction chamber (presumably for these two particular experiments,
871 sesquiterpenes and monoterpenes were present at concentrations below the detection
872 limits of the PTR-MS and CIR-TOF-MS). The concentration of camphore at lights on
873 was estimated to be ~ 0.5 – 0.9 ppbV for the *Ficus cyathistipula* system and ~ 1.4 –
874 2.7 ppbV for *Ficus benjamina,* and the sum of all *non-precursor* ions in the CIR-
875 TOF-MS mass spectrum > *m/z* 100 (indicative of *non-isoprene-like* oxidation
876 products; excluding *m/z* 103 and 117) was estimated to be of the order 2 ppbV by the
877 end of the experiments. This calculation approximates the *m/z* > 100 summation as
878 one large, multifunctional analyte with a PTR sensitivity similar to pinonaldehyde (a
879 typical, multifunctional, high MW molecule resulting from terpene oxidation).
880 Continuing this assumption and taking a range of known VOC terpene product yields

(Y^{P}_{VOC}) obtained from previous work at the Manchester chamber (i.e. Y^{P}_{VOC} = 100 % the limiting case; 77 % from *Ficus Benjamina* oxidation; 55 % from *Betula Pendula* oxidation; and 29 % for pinonaldehyde and $\Sigma(I_{111}, I_{93})$), a *non-isoprene* $VOC_{precursor}$ concentration may be estimated. Taking a range of known SOA yields obtained from the same reaction chamber (i.e. α-pinene, myrcene, linalool and β-caryophyllene; Alfarra et al., 2013), the SOA yield obtained here for the *Betula pendula* system and the estimate of [$VOC_{precursor}$], Eqn. (2) may be solved to provide a crude estimate of the mass of SOA formed from *non-isoprene* precursors. Consequently, an estimate of the residual SOA mass derived from isoprene oxidation within the *Ficus* system can be inferred for each of the experiments shown in Fig. 9.

For 78 of the 120 measurement-and-parameter sets tested, the estimated residual SOA mass resulting solely from isoprene oxidation was negative – i.e., production of SOA from isoprene oxidation was not required to close the mass balance. Values were calculated based on the widest range of peak masses observed during the *ficus* experiments (M_p = 1.3 μg m^{-3} and 5.5 μg m^{-3}), and assume the lowest (29 %) and highest (100 %) VOC terpene yields and lowest (5 %) and highest (47 %) SOA yields from non-isoprene precursors, respectively, as observed in previous experiments conducted within this chamber. These ranges result in calculated residual SOA mass of -28.5 to +5.0 μg m^{-3} produced solely from isoprene oxidation. Hence, there are combinations of measurements, observations and oxidation/phase-change parameters — omitting isoprene and its oxidation products — that can account for ~20 times the observed aerosol mass production, and other combinations of measurements and

903 parameters that leave up to ~ 90 % of the condensed mass to be explained by isoprene
904 oxidation. If, instead of using the limiting cases, the closest approximation to the *ficus*
905 *cyathistipula* system is used (i.e. Y_{VOC} = 77 % and $Y_{SOA} = Y_{SOA}$ = *a*-pinene = 15 %),
906 non-isoprene products could have accounted for around 145 % of the SOA mass that
907 was produced. We have no way of assigning formal likelihoods to each set of
908 measurements and parameters in this exercise, but we note that the great
909 preponderance of parameter combinations do not require an isoprene contribution to
910 the SOA mass (i.e. 78/120 measurement-and-parameter sets tested) under our
911 experimental conditions. Moreover, our experiments produce much less SOA mass
912 than would be expected from published experiments using individual mono- and
913 sesquiterpenes.

914 There are three principal reasons why the estimates of aerosol production from
915 isoprene in the tropical plant experiments span such a large range. Firstly, the plants
916 in the mesocosm emit a complicated mixture of biogenic VOCs, some of which are
917 known to oxidise much more rapidly than isoprene and which will produce
918 condensable compounds when oxidised. Secondly, these minor compounds co-
919 emitted from principally-isoprene emitting tropical trees are imperfectly quantified
920 because of the sensitivity of the chemical ionisation (PTR and CIR) instruments.
921 Thirdly, these minor co-emissions are imperfectly characterised because many higher
922 molecular weight compounds, such as the mono- and sesquiterpenes, are isobaric in
923 the PTR and CIR instruments and so precise chemical structures cannot easily be
924 assigned. Without better instrument detection sensitivity and high time resolution

chemical identification for the reactive compounds co-emitted with isoprene, it is not possible to constrain further the aerosol yield from the tropical plants. Unfortunately, insufficient SOA mass formed during *Ficus* experiments to allow us to conduct any form of compositional analysis.

4.3 Atmospheric significance

Our results are specific to VOC/NO_x ratios of 3 - 9 and NO_x mixing ratios of ~ 2 ppbV. Note, however, that the three reasons given above for the uncertainty in the aerosol production ascribed to isoprene in our experiments will also pertain to field measurements, often being exacerbated by variability and the difficulties of operating in the field. A contribution of isoprene to SOA is *supported* by recent observations of isoprene related SOA formation above the tropical forest of Danum Valley, Borneo, a high isoprene, low NO_x region (typical ratio of 20:1, isoprene/NO_x) (Hewitt et al., 2010b). Robinson *et al* (2010) observed that up to 15 % by mass of atmospheric sub-micron organic aerosol above the tropical forest of Danum Valley was comprised of methyl furan, the most likely source of which is the oxidation of isoprene (i.e. thermal decomposition of isoprene derived SOA) (Ruppert and Becker, 2000;Robinson et al., 2010; Lin et al., 2012; Budisulistiorini et al., 2013). Although much smaller in magnitude, the monoterpene emissions measured at Danum Valley were more than adequate to account for the remaining sub-micron organic aerosol (MacKenzie et al., 2011), just as in the majority of aerosol mass calculations for principally-isoprene-emitting tropical trees, described above.

946 It has recently been proposed that isoprene can inhibit aerosol formation when present
947 in air containing other potential SOA precursors, such as mono- and sesquiterpenes
948 (Kiendler-Scharr et al., 2009a). Kiendler-Scharr et al. propose that isoprene could
949 effectively act as an OH scavenger, suppressing new particle formation by slowing
950 the oxidation of available monoterpenes (and presumably sesquiterpenes). In line
951 with this thesis, interpretation of the results obtained from our seeded experiments
952 with *Ficus* species leaves room for a potential role for isoprene in inhibiting SOA
953 formation under certain atmospheric conditions, i.e. our results imply that isoprene
954 may impact negatively on the overall SOA forming potential of air containing other
955 biogenic SOA precursors. However, owing to the constraints laid upon our
956 experiments by the instrumentation and apparatus employed, it is difficult to assign a
957 given certainty level to the role played by isoprene in the ambient atmosphere and
958 caution should be taken when interpreting such findings.

959 The fact that isoprene accounts for approximately 50 % of the total global burden of
960 non-methane VOC, (Guenther et al., 2006), would make it a significant contributor to
961 global SOA. It has been estimated that, even if the secondary organic aerosol yield
962 from isoprene is small (e.g. 1 %), the overall contribution to total atmospheric aerosol
963 could be up to 6 Tg yr^{-1} (Carlton et al., 2009). Van Donkelaar *et al.* (2007) found that
964 using an isoprene SOA yield of 2 % improved the relationship between model
965 simulations and organic aerosol measurements, and contributed 10 – 50 % of the total
966 organic aerosol loading over the United States during the summer. Understanding the
967 exact role played by isoprene in air containing many different VOCs, and being able

968 to account for the differing isoprene SOA yields under contrasting NO_x and acidity
969 (Lin *et al.*, 2012; Lin *et al.*, 2013; Pye *et al.*, 2013) environments, will undoubtedly
970 help to significantly improve global modelling estimates of total SOA loading even
971 further (Couvidat and Seigneur, 2010).

972 Further to any such potential impacts imposed by isoprene, it has recently been shown
973 that a range of other BVOC emissions, released in response to a range of
974 environmental stress factors, can also have significant impacts on biogenic SOA
975 formation and yield (Mentel et al., 2013). It has been shown that the emissions of
976 sesquiterpenes, methyl salicylate and C_{17} BVOCs, released as a result of certain
977 environmental stress factors have a net positive impact on SOA yield; whereas certain
978 stress induced green leaf volatiles ((Z)-3-hexenol and (Z)-3-hexenylacetate) behave
979 similarly to isoprene, suppressing SOA formation (Mentel et al., 2013).

980 Given the highly differing reported yields of isoprene SOA under various oxidant
981 schemes, the uncertainty in the exact role played by isoprene and its oxidation
982 products in realistic mixtures of VOCs (in particular in the context of SOA nucleation
983 rates; Kiendler-Scharr et al., 2009a) and the lack of knowledge regarding stress
984 induced BVOCs, their atmospheric oxidation and their roles in biogenic SOA
985 formation (and impact on chemical and physical properties), we suggest that there is a
986 pressing requirement for additional, atmosphere-relevant laboratory and field studies
987 to give us the necessary insight to successfully control biogenic SOA (Carlton et al.,
988 2010).

Acknowledgements

The authors gratefully acknowledge the UK Natural Environment Research Council (NERC) for funding of the APPRAISE ACES (NE/E011217/1), ACIDPRUF (NE/I020121/1) and CLAIRE-UK (NE/I012567/1) consortia. The authors would also like to acknowledge support from the EU-FP7 EUROCHAMP-2 project. M. R. Alfarra was supported by UK National Centre for Atmospheric Sciences (NCAS) funding. The authors would like to thank Dr Iain White for his assistance with VOC measurements and instrument calibration. This is paper number 1 from the Birmingham Institute of Forest Research.

5 References

Alfarra, M. R., N. Good, K. P. Wyche, J. E. Hamilton, P. S. Monks, A. C. Lewis and G. McFiggans (2013). "Water uptake is independent of the inferred composition of secondary aerosols derived from multiple biogenic VOCs." Atmospheric Chemistry and Physics **13**(23): 11769-11789. DOI: 10.5194/acp-13-11769-2013.

Alfarra, M. R., J. F. Hamilton, K. P. Wyche, N. Good, M. W. Ward, T. Carr, M. H. Barley, P. S. Monks, M. E. Jenkin, A. C. Lewis and G. B. McFiggans (2012). "The effect of photochemical ageing and initial precursor concentration on the composition and hygroscopic properties of beta-caryophyllene secondary organic aerosol." Atmospheric Chemistry and Physics **12**(14): 6417-6436. DOI: 10.5194/acp-12-6417-2012.

Alfarra, M. R., D. Paulsen, M. Gysel, A. A. Garforth, J. Dommen, A. S. H. Prevot, D. R. Worsnop, U. Baltensperger and H. Coe (2006). "A mass spectrometric study of secondary organic aerosols formed from the photooxidation of anthropogenic and biogenic precursors in a reaction chamber." Atmospheric Chemistry and Physics **6**: 5279-5293.

1018 Alfarra, M. R., D. Paulsen, M. Gysel, A. A. Garforth, J. Dommen, A. S. H. Prévôt, D.
1019 R. Worsnop, U. Baltensperger and H. Coe (2006). "A mass spectrometric study of
1020 secondary organic aerosols formed from the photooxidation of anthropogenic and
1021 biogenic precursors in a reaction chamber." Atmospheric Chemistry and Physics **6**:
1022 5279–5293.
1023
1024 Atkinson, R. and J. Arey (2003). "Gas-phase tropospheric chemistry of biogenic
1025 volatile organic compounds: a review." Atmospheric Environment **37**: S197-S219.
1026 DOI: 10.1016/s1352-2310(03)00391-1.
1027
1028 Bahreini, R., M. D. Keywood, N. L. Ng, V. Varutbangkul, S. Gao, R. C. Flagan, J. H.
1029 Seinfeld, D. R. Worsnop and J. L. Jimenez (2005). "Measurements of secondary
1030 organic aerosol from oxidation of cycloalkenes, terpenes, and m-xylene using an
1031 Aerodyne aerosol mass spectrometer." Environmental Science and Technology, **39**:
1032 15, 5674-5688
1033
1034 Baltensperger, U., J. Dommen, R. Alfarra, J. Duplissy, K. Gaeggeler, A. Metzger, M.
1035 C. Facchini, S. Decesari, E. Finessi, C. Reinnig, M. Schott, J. Warnke, T. Hoffmann,
1036 B. Klatzer, H. Puxbaum, M. Geiser, M. Savi, D. Lang, M. Kalberer and T. Geiser
1037 (2008). "Combined determination of the chemical composition and of health effects
1038 of secondary organic aerosols: The POLYSOA project." Journal of Aerosol Medicine
1039 and Pulmonary Drug Delivery **21**(1): 145-154. DOI: 10.1089/jamp.2007.0655.
1040
1041 Benkelberg, H. J., O. Boge, R. Seuwen and P. Warneck (2000). "Product distributions
1042 from the OH radical-induced oxidation of but-1-ene, methyl-substituted but-1-enes
1043 and isoprene in NOx-free air." Physical Chemistry Chemical Physics **2**(18): 4029-
1044 4039. DOI: 10.1039/b002053m.
1045
1046 Blake, R. S., P. S. Monks and A. M. Ellis (2009). "Proton-Transfer Reaction Mass
1047 Spectrometry." Chemical Reviews **109**(3): 861-896. DOI: 10.1021/cr800364q.
1048
1049 Blake, R. S., C. Whyte, C. O. Hughes, A. M. Ellis and P. S. Monks (2004).
1050 "Demonstration of proton-transfer reaction time-of-flight mass spectrometry for real-
1051 time analysis of trace volatile organic compounds." Analytical Chemistry **76**(13):
1052 3841-3845. DOI: 10.1021/ac0498260.
1053
1054 Budisulistiorini, S. H., Canagaratna, M. R., Croteau, P. L., Marth, W. J., Baumann, K.,
1055 Edgerton, E. S., Shaw, S. L., Knipping, E. M., Worsnop, D. R., Jayne, J. T., Gold, A. and
1056 Surratt J. D.: Real-Time Continuous Characterization of Secondary Organic Aerosol
1057 Derived from Isoprene Epoxydiols in Downtown Atlanta, Georgia, Using the
1058 Aerodyne Aerosol Chemical Speciation Monitor, Environ. Sci. Technol., 47 (11), 686–
1059 5694, doi: 10.1021/es400023n, 2013

1060 Brégonzio-Rozier, L., Siekmann, F., Giorio, C., Pangui, E., Morales, S., B., Temime-Roussel,
1061 B., Gratien, A., Michoud, V., Ravier, S., Tapparo, A., Monod, A. and Doussin J.-F.: Gaseous
1062 products and Secondary Organic Aerosol formation during long term oxidation of isoprene
1063 and methacrolein, Atmos. Chem. Phys. Discuss., 14, 22507-22545, 2014

1064
1065 Camredon, M., J. F. Hamilton, M. S. Alam, K. P. Wyche, T. Carr, I. R. White, P. S.
1066 Monks, A. R. Rickard and W. J. Bloss (2010). "Distribution of gaseous and
1067 particulate organic composition during dark alpha-pinene ozonolysis." Atmospheric
1068 Chemistry and Physics **10**(6): 2893-2917.
1069
1070 Canagaratna, M. R., J. T. Jayne, J. L. Jimenez, J. D. Allan, M. R. Alfarra, Q. Zhang,
1071 T. B. Onasch, F. Drewnick, H. Coe, A. Middlebrook, A. Delia, L. R. Williams, A. M.
1072 Trimborn, M. J. Northway, P. F. DeCarlo, C. E. Kolb, P. Davidovits and D. R.
1073 Worsnop (2007). "Chemical and microphysical characterization of ambient aerosols
1074 with the aerodyne aerosol mass spectrometer." Mass Spectrometry Reviews **26**(2):
1075 185-222. DOI: :10.1002/mas.20115.
1076
1077 Carlton, A. G., R. W. Pinder, P. V. Bhave and G. A. Pouliot (2010). "To What Extent
1078 Can Biogenic SOA be Controlled?" Environmental Science & Technology **44**(9):
1079 3376-3380.
1080
1081 Carlton, A. G., C. Wiedinmyer and J. H. Kroll (2009). "A review of Secondary
1082 Organic Aerosol (SOA) formation from isoprene." Atmospheric Chemistry and
1083 Physics **9**(14): 4987-5005.
1084
1085 Carslaw, K. S., O. Boucher, D. V. Spracklen, G. W. Mann, J. G. L. Rae, S.
1086 Woodward and M. Kulmala (2010). "A review of natural aerosol interactions and
1087 feedbacks within the Earth system." Atmos. Chem. Phys. **10**(4): 1701-1737.
1088
1089 Carvalho, L. R. F., P. C. Vasconcellos, W. Mantovani, C. S. Pool and S. O. Pisani
1090 (2005). "Measurements of biogenic hydrocarbons and carbonyl compounds emitted
1091 by trees from temperate warm Atlantic rainforest, Brazil." Journal of Environmental
1092 Monitoring **7**(5): 493-499. DOI: 10.1039/b414881a.
1093
1094 Claeys, M., B. Graham, G. Vas, W. Wang, R. Vermeylen, V. Pashynska, J. Cafmeyer,
1095 P. Guyon, M. O. Andreae, P. Artaxo and W. Maenhaut (2004). "Formation of
1096 secondary organic aerosols through photooxidation of isoprene." Science **303**(5661):
1097 1173-1176.
1098
1099 Claeys, M., W. Wang, A. C. Ion, I. Kourtchev, A. Gelencser and W. Maenhaut
1100 (2004). "Formation of secondary organic aerosols from isoprene and its gas-phase
1101 oxidation products through reaction with hydrogen peroxide." Atmospheric
1102 Environment **38**(25): 4093-4098. DOI: 10.1016/j.atmosenv.2004.06.001.

Couvidat, F. and C. Seigneur (2010). "Modeling secondary organic aerosol formation from isoprene oxidation under dry and humid conditions." Atmos. Chem. Phys. Discuss. **10**(8): 20559-20605.

Dommen, J., H. HelleÌn, M. Saurer, M. Jaeggi, R. Siegwolf, A. Metzger, J. Duplissy, M. Fierz and U. Baltensperger (2009). "Determination of the Aerosol Yield of Isoprene in the Presence of an Organic Seed with Carbon Isotope Analysis." Environmental Science & Technology **43**(17): 6697-6702.

Donahue, N. M., A. L. Robinson and S. N. Pandis (2009). "Atmospheric organic particulate matter: From smoke to secondary organic aerosol." Atmospheric Environment **43**(1): 94-106.

Drewnick, F., S. S. Hings, P. DeCarlo, J. T. Jayne, M. Gonin, K. Fuhrer, S. Weimer, J. L. Jimenez, K. L. Demerjian, S. Borrmann and D. R. Worsnop (2005). "A new time-of-flight aerosol mass spectrometer (TOF-AMS) - Instrument description and first field deployment." Aerosol Science and Technology **39**(7): 637-658. DOI: 10.1080/02786820500182040.

Ehn, M., Thornton, J. A., Kleist, E., Sipila, M., Junninen, H., Pullinen, I., Springer, M., Rubach, F., Tillmann, R., Lee, B., Lopez-Hilfiker, F., Andres, S., Acir, I. H., Rissanen, M., Jokinen, T., Schobesberger, S., Kangasluoma, J., Kontkanen, J., Nieminen, T., Kurten, T., Nielsen, L. B., Jorgensen, S., Kjaergaard, H. G., Canagaratna, M., Dal Maso, M., Berndt, T., Petaja, T.,Wahner, A., Kerminen, V. M., Kulmala, M., Worsnop, D. R., Wildt, J., and Mentel, T. F.: A large source of low-volatility secondary organic aerosol, Nature, 506 (7489), 476-479, doi: 10.1038/nature13032, 2014

Edney, E. O., T. E. Kleindienst, M. Jaoui, M. Lewandowski, J. H. Offenberg, W. Wang and M. Claeys (2005). "Formation of 2-methyl tetrols and 2-methylglyceric acid in secondary organic aerosol from laboratory irradiated isoprene/NOX/SO2/air mixtures and their detection in ambient PM2.5 samples collected in the eastern United States." Atmospheric Environment **39**(29): 5281-5289. DOI: 10.1016/j.atmosenv.2005.05.031.

Geron, C., S. Owen, A. Guenther, J. Greenberg, R. Rasmussen, J. Hui Bai, Q.-J. Li and B. Baker (2006). "Volatile organic compounds from vegetation in southern Yunnan Province, China: Emission rates and some potential regional implications." Atmospheric Environment **40**(10): 1759-1773.

1144 Guenther, A., T. Karl, P. Harley, C. Wiedinmyer, P. I. Palmer and C. Geron (2006).
1145 "Estimates of global terrestrial isoprene emissions using MEGAN (Model of
1146 Emissions of Gases and Aerosols from Nature)." Atmospheric Chemistry and Physics
1147 **6**: 3181-3210.
1148
1149 Guenther, A. B., X. Jiang, C. L. Heald, T. Sakulyanontvittaya, T. Duhl, L. K.
1150 Emmons and X. Wang (2012). "The Model of Emissions of Gases and Aerosols from
1151 Nature version 2.1 (MEGAN2.1): an extended and updated framework for modeling
1152 biogenic emissions." Geosci. Model Dev. **5**(6): 1471-1492. DOI: 10.5194/gmd-5-
1153 1471-2012.
1154
1155 Gunthe, S. S., S. M. King, D. Rose, Q. Chen, P. Roldin, D. K. Farmer, J. L. Jimenez,
1156 P. Artaxo, M. O. Andreae, S. T. Martin and U. Poschl (2009). "Cloud condensation
1157 nuclei in pristine tropical rainforest air of Amazonia: size-resolved measurements and
1158 modeling of atmospheric aerosol composition and CCN activity." Atmospheric
1159 Chemistry and Physics **9**(19): 7551-7575.
1160
1161 Hallquist, M., J. C. Wenger, U. Baltensperger, Y. Rudich, D. Simpson, M. Claeys, J.
1162 Dommen, N. M. Donahue, C. George, A. H. Goldstein, J. F. Hamilton, H. Herrmann,
1163 T. Hoffmann, Y. Iinuma, M. Jang, M. E. Jenkin, J. L. Jimenez, A. Kiendler-Scharr,
1164 W. Maenhaut, G. McFiggans, T. F. Mentel, A. Monod, A. S. H. Prevot, J. H. Seinfeld,
1165 J. D. Surratt, R. Szmigielski and J. Wildt (2009). "The formation, properties and
1166 impact of secondary organic aerosol: current and emerging issues." Atmospheric
1167 Chemistry and Physics **9**(14): 5155-5236.
1168
1169 Hamilton, J. F., Alfarra, M. R., Robinson, N., Ward, M. W., Lewis, A. C.,
1170 McFiggans, G. B., Coe, H., and Allan, J. D.: Linking biogenic hydrocarbons to
1171 biogenic aerosol in the Borneo rainforest. Atmos. Chem. Phys., 13(22), 11295-11305,
1172 doi:10.5194/acp-13-11295-2013, 2013.

1173 Healy, R. M., J. C. Wenger, A. Metzger, J. Duplissy, M. Kalberer and J. Dommen
1174 (2008). "Gas/particle partitioning of carbonyls in the photooxidation of isoprene and
1175 1,3,5-trimethylbenzene." Atmospheric Chemistry and Physics **8**(12): 3215-3230.
1176
1177 Hewitt, C. N., J. D. Lee, A. R. MacKenzie, M. P. Barkley, N. Carslaw, G. D. Carver,
1178 N. A. Chappell, H. Coe, C. Collier, R. Commane, F. Davies, B. Davison, P. Di Carlo,
1179 C. F. Di Marco, J. R. Dorsey, P. M. Edwards, M. J. Evans, D. Fowler, K. L.
1180 Furneaux, M. Gallagher, A. Guenther, D. E. Heard, C. Helfter, J. Hopkins, T. Ingham,
1181 M. Irwin, C. Jones, A. Karunaharan, B. Langford, A. C. Lewis, S. F. Lim, S. M.
1182 MacDonald, A. S. Mahajan, S. Malpass, G. McFiggans, G. Mills, P. Misztal, S.
1183 Moller, P. S. Monks, E. Nemitz, V. Nicolas-Perea, H. Oetjen, D. E. Oram, P. I.
1184 Palmer, G. J. Phillips, R. Pike, J. M. C. Plane, T. Pugh, J. A. Pyle, C. E. Reeves, N. H.
1185 Robinson, D. Stewart, D. Stone, L. K. Whalley and X. Yin (2010). "Overview:

oxidant and particle photochemical processes above a south-east Asian tropical rainforest (the OP3 project): introduction, rationale, location characteristics and tools." Atmospheric Chemistry and Physics **10**(1): 169-199.

Hewitt, C. N., J. D. Lee, A. R. MacKenzie, M. P. Barkley, N. Carslaw, G. D. Carver, N. A. Chappell, H. Coe, C. Collier, R. Commane, F. Davies, B. Davison, P. DiCarlo, C. F. Di Marco, J. R. Dorsey, P. M. Edwards, M. J. Evans, D. Fowler, K. L. Furneaux, M. Gallagher, A. Guenther, D. E. Heard, C. Helfter, J. Hopkins, T. Ingham, M. Irwin, C. Jones, A. Karunaharan, B. Langford, A. C. Lewis, S. F. Lim, S. M. MacDonald, A. S. Mahajan, S. Malpass, G. McFiggans, G. Mills, P. Misztal, S. Moller, P. S. Monks, E. Nemitz, V. Nicolas-Perea, H. Oetjen, D. E. Oram, P. I. Palmer, G. J. Phillips, R. Pike, J. M. C. Plane, T. Pugh, J. A. Pyle, C. E. Reeves, N. H. Robinson, D. Stewart, D. Stone, L. K. Whalley and X. Yin (2010). "Overview: oxidant and particle photochemical processes above a south-east Asian tropical rainforest (the OP3 project): introduction, rationale, location characteristics and tools." Atmos. Chem. Phys. **10**(1): 169-199.

Holzinger, R., A. Lee, K. T. Paw and A. H. Goldstein (2005). "Observations of oxidation products above a forest imply biogenic emissions of very reactive compounds." Atmospheric Chemistry and Physics **5**: 67-75.

Pye, H. O. T., Pinder, R. W., Piletic, I. R., Xie, Y., Capps, S. L., Lin, Y. H., Surratt, J. D., Zhang, Z., Gold, A., Luecken, D. J., Hutzell, W. T., Jaoui, J., Offenberg, J. H., Kleindienst, T. E., Lewandowski, M., and Edney E. O.: Epoxide Pathways Improve Model Predictions of Isoprene Markers and Reveal Key Role of Acidity in Aerosol Formation, Environ. Sci. Technol., 47 (19), 11056–11064, doi: 10.1021/es402106h, 2013

IPCC (2007). Climate change 2007: The Physical Science Basis, Cambridge University Press, Cambridge.

Isaksen, I. S. A., C. Granier, G. Myhre, T. K. Berntsen, S. B. Dalsoren, M. Gauss, Z. Klimont, R. Benestad, P. Bousquet, W. Collins, T. Cox, V. Eyring, D. Fowler, S. Fuzzi, P. Jockel, P. Laj, U. Lohmann, M. Maione, P. Monks, A. S. H. Prevot, F. Raes, A. Richter, B. Rognerud, M. Schulz, D. Shindell, D. S. Stevenson, T. Storelvmo, W. C. Wang, M. van Weele, M. Wild and D. Wuebbles (2009). "Atmospheric composition change: Climate-Chemistry interactions." Atmospheric Environment **43**(33): 5138-5192. DOI: 10.1016/j.atmosenv.2009.08.003.

Jang, M. S., N. M. Czoschke, S. Lee and R. M. Kamens (2002). "Heterogeneous atmospheric aerosol production by acid-catalyzed particle-phase reactions." Science, 298, 814-817.

Jaoui, M., E. W. Corse, M. Lewandowski, J. H. Offenberg, T. E. Kleindienst and E. O. Edney (2010). "Formation of organic tracers for isoprene SOA under acidic conditions." Atmospheric Environment **In Press, Corrected Proof**.

Jenkin, M. E., S. M. Saunders, and M. J. Pilling (1997). "The tropospheric degradation of volatile organic compounds: a protocol for mechanism development." Atmospheric Environment **31**(1): 81-104, 1997.

Jenkin, M. E. (2004). "Modelling the formation and composition of secondary organic aerosol from alpha- and beta-pinene ozonolysis using MCM v3." Atmospheric Chemistry and Physics **4**: 1741-1757.

Jenkin, M. E., K. P. Wyche, C. J. Evans, T. Carr, P. S. Monks, M. R. Alfarra, M. H. Barley, G. B. McFiggans, J. C. Young and A. R. Rickard (2012). "Development and chamber evaluation of the MCM v3.2 degradation scheme for beta-caryophyllene." Atmospheric Chemistry and Physics **12**(11): 5275-5308. DOI: 10.5194/acp-12-5275-2012.

Junkermann, W., J. Hacker, T. Lyons and U. Nair (2009). "Land use change suppresses precipitation." Atmospheric Chemistry and Physics **9**(17): 6531-6539.

Kanawade, V. P., B. T. Jobson, A. B. Guenther, M. E. Erupe, S. N. Pressley, S. N. Tripathi and S. H. Lee (2011). "Isoprene suppression of new particle formation in a mixed deciduous forest." Atmospheric Chemistry and Physics **11**(12): 6013-6027.

Karl, M., K. Tsigaridis, E. Vignati and F. Dentener (2009). "Formation of secondary organic aerosol from isoprene oxidation over Europe." Atmospheric Chemistry and Physics **9**(18): 7003-7030.

Kiendler-Scharr, A., J. Wildt, M. Dal Maso, T. Hohaus, E. Kleist, T. F. Mentel, R. Tillmann, R. Uerlings, U. Schurr and A. Wahner (2009a). "New particle formation in forests inhibited by isoprene emissions." Nature **461**(7262): 381-384. DOI: 10.1038/nature08292.

Kiendler-Scharr, A., Q. Zhang, T. Hohaus, E. Kleist, A. Mensah, T. F. Mentel, C. Spindler, R. Uerlings, R. Tillmann and J. Wildt (2009b). "Aerosol Mass Spectrometric Features of Biogenic SOA: Observations from a Plant Chamber and in Rural Atmospheric Environments." Environmental Science & Technology **43**(21): 8166-8172.

Kim, D. Y. and V. Ramanathan (2008). "Solar radiation budget and radiative forcing due to aerosols and clouds." Journal of Geophysical Research-Atmospheres **113**(D2).

Kim, S., A. Guenther, T. Karl and J. Greenberg (2011). "Contributions of primary and secondary biogenic VOC to total OH reactivity during CABINEX (Community Atmosphere-Biosphere INteractions Experiments)-09 field campaign." Atmospheric Chemistry and Physics **11**: 8613-8623.

Kleindienst, T. E., E. O. Edney, M. Lewandowski, J. H. Offenberg and M. Jaoui (2006). "Secondary organic carbon and aerosol yields from the irradiations of isoprene and alpha-pinene in the presence of NOx and SO2." Environmental Science & Technology **40**(12): 3807-3812.

Kleindienst, T. E., M. Lewandowski, J. H. Offenberg, M. Jaoui and E. O. Edney (2007). "Ozone-isoprene reaction: Re-examination of the formation of secondary organic aerosol." Geophysical Research Letters **34**(1).

Kleindienst, T. E., M. Lewandowski, J. H. Offenberg, M. Jaoui and E. O. Edney (2009). "The formation of secondary organic aerosol from the isoprene plus OH reaction in the absence of NOx." Atmospheric Chemistry and Physics **9**(17): 6541-6558.

Kokkola, H., P. Yli-Pirila, M. Vesterinen, H. Korhonen, H. Keskinen, S. Romakkaniemi, L. Hao, A. Kortelainen, J. Joutsensaari, D. R. Worsnop, A. Virtanen and K. E. J. Lehtinen (2014). "The role of low volatile organics on secondary organic aerosol formation." Atmospheric Chemistry and Physics **14**(3): 1689-1700. DOI: 10.5194/acp-14-1689-2014.

Kroll, J. H., N. L. Ng, S. M. Murphy, R. C. Flagan and J. H. Seinfeld (2005). "Secondary organic aerosol formation from isoprene photooxidation under high-NOx conditions." Geophysical Research Letters **32**(18). DOI: 10.1029/2005gl023637.

Kroll, J. H., N. L. Ng, S. M. Murphy, R. C. Flagan and J. H. Seinfeld (2006). "Secondary organic aerosol formation from isoprene photooxidation." Environmental Science & Technology **40**(6): 1869-1877. DOI: 10.1021/es0524301.

Lee, A., A. H. Goldstein, J. H. Kroll, N. L. Ng, V. Varutbangkul, R. C. Flagan and J. H. Seinfeld (2006a). "Gas-phase products and secondary aerosol yields from the photooxidation of 16 different terpenes." Journal of Geophysical Research-Atmospheres **111**(D17). DOI: 10.1029/2006jd007050.

Lee, A., A. H. Goldstein, M. D. Keywood, S. Gao, V. Varutbangkul, R. Bahreini, N. L. Ng, R. C. Flagan and J. H. Seinfeld (2006b). "Gas-phase products and secondary aerosol yields from the ozonolysis of ten different terpenes." Journal of Geophysical Research-Atmospheres **111**(D17). D07302, DOI:10.1029/2005JD006437.

Liggio, J., S. M. Li, J. R. Brook and C. Mihele (2007). "Direct polymerization of isoprene and α-pinene on acidic aerosols." Geophysical Research Letters, 34, L05814, 10.1029/2006gl028468.

Limbeck, A., M. Kulmala and H. Puxbaum (2003). "Secondary organic aerosol formation in the atmosphere via heterogeneous reaction of gaseous isoprene on acidic particles." Geophysical Research Letters, 30, 1996, 10.1029/2003gl017738.

Lin, P., J. Z. Yu, G. Engling and M. Kalberer (2012). "Organosulfates in Humic-like Substance Fraction Isolated from Aerosols at Seven Locations in East Asia: A Study by Ultra-High-Resolution Mass Spectrometry." Environmental Science & Technology, 46, 13118-13127, 10.1021/es303570v.

Lin, Y. H., Zhang, Z., Docherty, K. S., Zhang, H., Budisulistiorini, S. H., Rubitschun, C. L., Shaw, S. L., Knipping, E. M., Edgerton, E. S., Kleindienst, T. E., Gold, A., and Surratt, J. D.: Isoprene Epoxydiols as Precursors to Secondary Organic Aerosol Formation: Acid-Catalyzed Reactive Uptake Studies with Authentic Compounds, Environ. Sci. Technol., 46 (1), 250–258, doi: 10.1021/es202554c, 2012

Lin, Y.-H., H. Zhang, H. O. T. Pye, Z. Zhang, W. J. Marth, S. Park, M. Arashiro, T. Cui, S. H. Budisulistiorini, K. G. Sexton, W. Vizuete, Y. Xie, D. J. Luecken, I. R. Piletic, E. O. Edney, L. J. Bartolotti, A. Gold and J. D. Surratt (2013). "Epoxide as a precursor to secondary organic aerosol formation from isoprene photooxidation in the presence of nitrogen oxides." Proceedings of the National Academy of Sciences, 110, 6718-6723, 10.1073/pnas.1221150110.

Lin, Y. H., Knipping, E. M., Edgerton, E. S., Shaw, S. L., and Surratt, J. D.: Investigating the influences of SO_2 and NH_3 levels on isoprene-derived secondary organic aerosol formation using conditional sampling approaches, Atmos. Chem. Phys., 13, 8457-8470, doi: 10.5194/acp-13-8457-2013, 2013

MacKenzie, A. R., B. Langford, T. A. M. Pugh, N. Robinson, P. K. Misztal, D. E. Heard, J. D. Lee, A. C. Lewis, C. E. Jones, J. R. Hopkins, G. Phillips, P. S. Monks, A. Karunaharan, K. E. Hornsby, V. Nicolas-Perea, H. Coe, A. M. Gabey, M. W. Gallagher, L. K. Whalley, P. M. Edwards, M. J. Evans, D. Stone, T. Ingham, R. Commane, K. L. Furneaux, J. B. McQuaid, E. Nemitz, Y. K. Seng, D. Fowler, J. A. Pyle and C. N. Hewitt (2011). "The atmospheric chemistry of trace gases and particulate matter emitted by different land uses in Borneo." Philosophical Transactions of the Royal Society B-Biological Sciences **366**(1582): 3177-3195. DOI: 10.1098/rstb.2011.0053.

Matsunaga, A. and P. J. Ziemann (2010). "Gas-Wall Partitioning of Organic Compounds in a Teflon Film Chamber and Potential Effects on Reaction Product and

Aerosol Yield Measurements." Aerosol Science and Technology **44**(10): 881-892. DOI: 10.1080/02786826.2010.501044.

Mentel, T. F., E. Kleist, S. Andres, M. Dal Maso, T. Hohaus, A. Kiendler-Scharr, Y. Rudich, M. Springer, R. Tillmann, R. Uerlings, A. Wahner and J. Wildt (2013). "Secondary aerosol formation from stress-induced biogenic emissions and possible climate feedbacks." Atmospheric Chemistry and Physics **13**(17): 8755-8770. DOI: 10.5194/acp-13-8755-2013.

Mentel, T. F., J. Wildt, A. Kiendler-Scharr, E. Kleist, R. Tillmann, M. Dal Maso, R. Fisseha, T. Hohaus, H. Spahn, R. Uerlings, R. Wegener, P. T. Griffiths, E. Dinar, Y. Rudich and A. Wahner (2009). "Photochemical production of aerosols from real plant emissions." Atmospheric Chemistry and Physics **9**(13): 4387-4406.

Mercado, L. M., N. Bellouin, S. Sitch, O. Boucher, C. Huntingford, M. Wild and P. M. Cox (2009). "Impact of changes in diffuse radiation on the global land carbon sink." Nature **458**(7241): 1014-U1087.

Meyer, N. K., J. Duplissy, M. Gysel, A. Metzger, J. Dommen, E. Weingartner, M. R. Alfarra, A. S. H. Prevot, C. Fletcher, N. Good, G. McFiggans, A. M. Jonsson, M. Hallquist, U. Baltensperger and Z. D. Ristovski (2009). "Analysis of the hygroscopic and volatile properties of ammonium sulphate seeded and unseeded SOA particles." Atmospheric Chemistry and Physics **9**(2): 721-732.

Ng, N. L., J. H. Kroll, M. D. Keywood, R. Bahreini, V. Varutbangkul, R. C. Flagan, J. H. Seinfeld, A. Lee and A. H. Goldstein (2006). "Contribution of first- versus second-generation products to secondary organic aerosols formed in the oxidation of biogenic hydrocarbons." Environmental Science & Technology **40**(7): 2283-2297. DOI: 10.1021/es052269u.

Paulot, F., J. D. Crounse, H. G. Kjaergaard, A. Kurten, J. M. St Clair, J. H. Seinfeld and P. O. Wennberg (2009). "Unexpected Epoxide Formation in the Gas-Phase Photooxidation of Isoprene." Science **325**(5941): 730-733. DOI: 10.1126/science.1172910.

Paulson, S. E. and J. H. Seinfeld (1992). "DEVELOPMENT AND EVALUATION OF A PHOTOOXIDATION MECHANISM FOR ISOPRENE." Journal of Geophysical Research-Atmospheres **97**(D18): 20703-20715.

Riipinen, I., T. Yli-Juuti, J. R. Pierce, T. Petaja, D. R. Worsnop, M. Kulmala and N. M. Donahue (2012). "The contribution of organics to atmospheric nanoparticle growth." Nature Geosci **5**(7): 453-458.

1400 Robinson, N. H., J. F. Hamilton, J. D. Allan, B. Langford, D. E. Oram, Q. Chen, K.
1401 Docherty, D. K. Farmer, J. L. Jimenez, M. W. Ward, C. N. Hewitt, M. H. Barley, M.
1402 E. Jenkin, A. R. Rickard, S. T. Martin, G. McFiggans and H. Coe (2010). "Evidence
1403 for a significant proportion of Secondary Organic Aerosol from isoprene above a
1404 maritime tropical forest." Atmos. Chem. Phys. Discuss. **10**(11): 25545-25576.
1405
1406 Robinson, N. H., J. F. Hamilton, J. D. Allan, B. Langford, D. E. Oram, Q. Chen, K.
1407 Docherty, D. K. Farmer, J. L. Jimenez, M. W. Ward, C. N. Hewitt, M. H. Barley, M.
1408 E. Jenkin, A. R. Rickard, S. T. Martin, G. McFiggans and H. Coe (2011). "Evidence
1409 for a significant proportion of Secondary Organic Aerosol from isoprene above a
1410 maritime tropical forest." Atmospheric Chemistry and Physics **11**(3): 1039-1050.
1411 DOI: 10.5194/acp-11-1039-2011.
1412
1413 Rollins, A. W., A. Kiendler-Scharr, J. L. Fry, T. Brauers, S. S. Brown, H. P. Dorn, W.
1414 P. Dube, H. Fuchs, A. Mensah, T. F. Mentel, F. Rohrer, R. Tillmann, R. Wegener, P.
1415 J. Wooldridge and R. C. Cohen (2009). "Isoprene oxidation by nitrate radical: alkyl
1416 nitrate and secondary organic aerosol yields." Atmospheric Chemistry and Physics
1417 **9**(18): 6685-6703.
1418
1419 Ruppert, L. and K. H. Becker (2000). "A product study of the OH radical-initiated
1420 oxidation of isoprene: formation of C-5-unsaturated diols." Atmospheric Environment
1421 **34**(10): 1529-1542.
1422
1423 Sillman, S. (1999). "The relation between ozone, NOx and hydrocarbons in urban and
1424 polluted rural environments." Atmospheric Environment **33**(12): 1821-1845.
1425
1426 Sprengnether, M., K. L. Demerjian, N. M. Donahue and J. G. Anderson (2002).
1427 "Product analysis of the OH oxidation of isoprene and 1,3-butadiene in the presence
1428 of NO." Journal of Geophysical Research-Atmospheres **107**(D15). DOI:
1429 10.1029/2001jd000716.
1430
1431 Stevens, B. and G. Feingold (2009). "Untangling aerosol effects on clouds and
1432 precipitation in a buffered system." Nature **461**(7264): 607-613.
1433
1434 Surratt, J. D., A. W. H. Chan, N. C. Eddingsaas, M. Chan, C. L. Loza, A. J. Kwan, S.
1435 P. Hersey, R. C. Flagan, P. O. Wennberg and J. H. Seinfeld (2010). "Reactive
1436 intermediates revealed in secondary organic aerosol formation from isoprene."
1437 Proceedings of the National Academy of Sciences **107**(15): 6640-6645. DOI:
1438 10.1073/pnas.0911114107.
1439
1440 Surratt, J. D., M. Lewandowski, J. H. Offenberg, M. Jaoui, T. E. Kleindienst, E. O.
1441 Edney and J. H. Seinfeld (2007). "Effect of Acidity on Secondary Organic Aerosol
1442 Formation from Isoprene." Environmental Science & Technology **41**(15): 5363-5369.
1443

Surratt, J. D., S. M. Murphy, J. H. Kroll, N. L. Ng, L. Hildebrandt, A. Sorooshian, R. Szmigielski, R. Vermeylen, W. Maenhaut, M. Claeys, R. C. Flagan and J. H. Seinfeld (2006). "Chemical composition of secondary organic aerosol formed from the photooxidation of isoprene." Journal of Physical Chemistry A **110**(31): 9665-9690. DOI: 10.1021/jp061734m.

Surratt, J. D., S. M. Murphy, J. H. Kroll, N. L. Ng, L. Hildebrandt, A. Sorooshian, R. Szmigielski, R. Vermeylen, W. Maenhaut, M. Claeys, R. C. Flagan and J. H. Seinfeld (2006). "Chemical Composition of Secondary Organic Aerosol Formed from the Photooxidation of Isoprene." The Journal of Physical Chemistry A **110**(31): 9665-9690.

Surratt, J. D., A. W. H. Chan, N. C. Eddingsaas, M. Chan, C. L. Loza, A. J. Kwan, S. P. Hersey, R. C. Flagan, P. O. Wennberg and J. H. Seinfeld (2010). "Reactive intermediates revealed in secondary organic aerosol formation from isoprene." Proceedings of the National Academy of Sciences, 107, 6640-6645, 10.1073/pnas.0911114107, 2010.

Tuazon, E. C. and R. Atkinson (1990). "A PRODUCT STUDY OF THE GAS-PHASE REACTION OF ISOPRENE WITH THE OH RADICAL IN THE PRESENCE OF NOX." International Journal of Chemical Kinetics **22**(12): 1221-1236. DOI: 10.1002/kin.550221202.

van Donkelaar, A., R. V. Martin, R. J. Park, C. L. Heald, T. M. Fu, H. Liao and A. Guenther (2007). "Model evidence for a significant source of secondary organic aerosol from isoprene." Atmospheric Environment **41**(6): 1267-1274. DOI: 10.1016/j.atmosenv.2006.09.051.

VanReken, T. M., J. P. Greenberg, P. C. Harley, A. B. Guenther and J. N. Smith (2006). "Direct measurement of particle formation and growth from the oxidation of biogenic emissions." Atmospheric Chemistry and Physics **6**: 4403-4413.

Verheggen, B. and M. Mozurkewich (2006). "An inverse modeling procedure to determine particle growth and nucleation rates from measured aerosol size distributions." Atmos. Chem. Phys., 6, 2927-2942, doi:10.5194/acp-6-2927-2006.

Virtanen, A., J. Joutsensaari, T. Koop, J. Kannosto, P. Yli-Pirila, J. Leskinen, J. M. Makela, J. K. Holopainen, U. Poschl, M. Kulmala, D. R. Worsnop and A. Laaksonen (2010). "An amorphous solid state of biogenic secondary organic aerosol particles." Nature **467**(7317): 824-827.

Wang, W., G. Vas, R. Dommisse, K. Loones and M. Claeys (2004). "Fragmentation study of diastereoisomeric 2-methyltetrols, oxidation products of isoprene, as their

trimethylsilyl ethers, using gas chromatography/ion trap mass spectrometry." Rapid Communications in Mass Spectrometry **18**(16): 1787-1797. DOI: 10.1002/rcm.1553.

Wyche, K. P., R. S. Blake, A. M. Ellis, P. S. Monks, T. Brauers, R. Koppmann and E. C. Apel (2007). "Technical note: Performance of Chemical Ionization Reaction Time-of-Flight Mass Spectrometry (CIR-TOF-MS) for the measurement of atmospherically significant oxygenated volatile organic compounds." Atmospheric Chemistry and Physics **7**: 609-620.

Wyche, K. P., et al. (2014) "Mapping organic reactivity during secondary organic aerosol formation". **In Preparation**.

Zhang, Q., J. L. Jimenez, M. R. Canagaratna, J. D. Allan, H. Coe, I. Ulbrich, M. R. Alfarra, A. Takami, A. M. Middlebrook, Y. L. Sun, K. Dzepina, E. Dunlea, K. Docherty, P. F. DeCarlo, D. Salcedo, T. Onasch, J. T. Jayne, T. Miyoshi, A. Shimono, S. Hatakeyama, N. Takegawa, Y. Kondo, J. Schneider, F. Drewnick, S. Borrmann, S. Weimer, K. Demerjian, P. Williams, K. Bower, R. Bahreini, L. Cottrell, R. J. Griffin, J. Rautiainen, J. Y. Sun, Y. M. Zhang and D. R. Worsnop (2007). "Ubiquity and dominance of oxygenated species in organic aerosols in anthropogenically-influenced Northern Hemisphere midlatitudes." Geophysical Research Letters **34**(13). DOI: 10.1029/2007gl029979.

Zhao, J., R. Zhang, E. C. Fortner and S. W. North (2004). "Quantification of hydroxycarbonyls from OH-isoprene reactions." Journal of the American Chemical Society **126**: 2686-2687.

1512 **Tables**

1513 Table 1: List of experiments conducted and their general parameters

Date	Tree Species	Initial NO_x / ppbV	VOC/NO_x	Relative Humidity / %	Pre-existing Seed
22/06/09	*Ficus benjamina*	3	4.2	79	None
23/06/09	*Ficus benjamina*	6	2.7	75	None
25/06/09	*Ficus benjamina*	2	6.3	65	Sulphate
29/06/09	*Ficus cyathistipula*	2	9.4	71	None
30/06/09	*Ficus cyathistipula*	2	7.8	75	Sulphate
02/07/09	*Ficus cyathistipula*	3	5.6	78	Sulphate
06/07/09	*Betula pendula*	3	5.6	84	None
07/07/09	*Betula pendula*	3	5.5	73	Sulphate
09/07/09	*Betula pendula*	2	1.5	70	Sulphate
10/07/09	*Betula pendula* + 36 ppbV isoprene	2	5.5	70	Sulphate
13/07/09	*Ficus benjamina*	2	-[1]	87	Sulphate
15/07/09	*Ficus benjamina*	3	-[1]	89	Sulphate

16/07/09	*Ficus benjamina* + 4.5 ppbV limonene	2	-[1]	85	None

Notes:

1. No quantified VOC data available

1517

1518 Table 2: GC-MS identification of the biogenic VOC present in the plant chamber air
1519 immediately before RC filling began. Quantification of isoprene, total monoterpenes
1520 and total sesquiterpenes was carried out using PTR-MS and CIRMS (see Figures 2
1521 and 5).

Experiment	Compounds detected by GC-MS (abundance ppbV) (trace = <0.1 ppb)			
	Isoprene	Monoterpenes (and related)	Sesquiterpenes	Other
B. Pendula	Yes (0.25-1.19)	α-pinene (0.31 – 1.08) β-pinene (0.74 – 7.19) ocimene (trace – 1.22) Δ3-carene (1.89 – 4.94) γ-terpinene (trace) 2, 4, 6-octatriene,2,6-dimethyl (trace) 4,7-methano-1H-indene, octahydro (trace)	β-caryophyllene (0.15 – 0.22) α-farnesene (0.14) α-caryophyllene (0.59 – 0.92) α-copaene (trace) aromadendrene (0.45-0.51) α-cedrene (trace) α-pyronene (trace)	acetaldehyde (trace) caryophyllene-epoxide (trace) nerolidol (trace) linalool (trace)

F. Benjamina	Yes (38.49)	α-pinene (trace) limonene (trace) sabinene (trace) linalool (trace)	α-cubebene (trace)	acetaldehyde (trace) benzoquinone (trace) pyridine (trace) methyl salicate (trace) decanal (trace)
F. Cyathistipula	Yes (75.08)	α-pinene (trace) β-pinene (trace) limonene (trace)	β-caryophyllene (trace)	acetic acid (trace)
Mixed canopy *F. Benjamina* *F. Cyathistipula* *C. Millis*	Yes	α-pinene (0.37) camphene (0.11) limonene (0.42) ocimene (trace)	None detected	*p*-dichlorobenzene methyl salicate

1522

1523

1524

1525

1526

1526

1527 Table 3: Yields of isoprene oxidation products compared to literature values. Yields
1528 are an average from all *Ficus* experiments (seeded and unseeded) (n = 4) calculated at
1529 4 hours after lights on (HALO). Yield is based on the calculated relationship between
1530 the amount of isoprene reacted and the oxidation product in question.

1531

Isoprene	Hydro-peroxides[1]	MVK +MACR	Hydroxy-acetone	Form-aldehyde	Source
1	0.33	0.26	0.07		Williams et al 1999
1	0.05	0.36	0.05		Williams et al 2001 (NO_x present)
1		0.33		0.67	Zang et al 2002
1		0.46 – 0.60		0.86 – 0.96	Niki et al 1983 Kamens et al 1982
1	0.18	0.25			Surratt et al 2010 NO_x present NO_x absent
1		0.27			Kleindienst et al 2009
1	0.01 –	0.17 – 0.36	0 – 0.02	0.02 – 0.07	This study

Isoprene	Hydro-peroxides[1]	MVK +MACR	Hydroxy-acetone	Form-aldehyde	Source
	0.03				

1532

1533 Notes:

1534 1. Sum of isoprene epoxide (IEPOX) and isoprene hydroperoxide (ISOPOOH)

1535

Figures

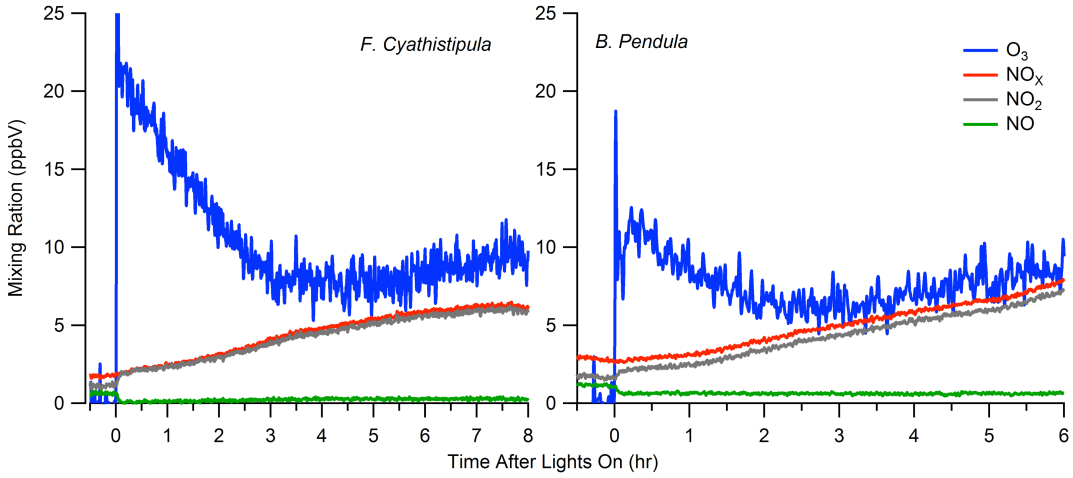

Figure 1: Temporal evolution of NO, NO_2, NO_x and O_3 during typical *Ficus Cyathistipula* (a) and *Betula pendula* (b) experiments (25/06/09 and 07/07/09, respectively).

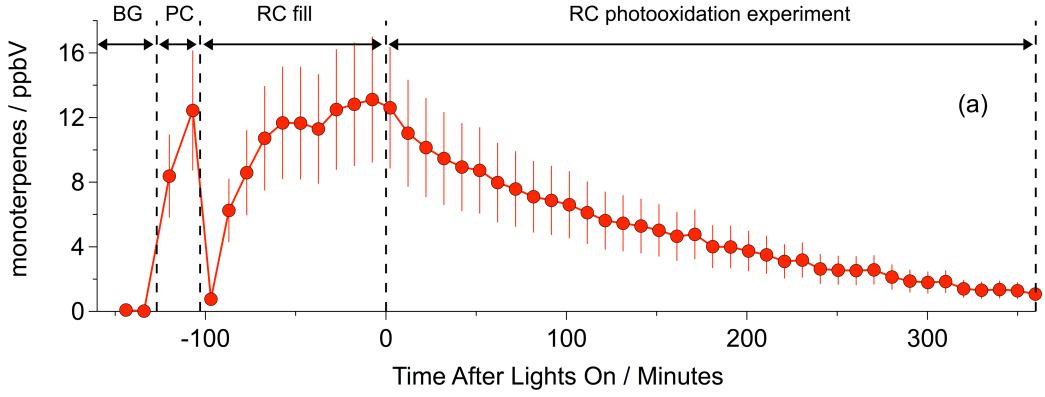

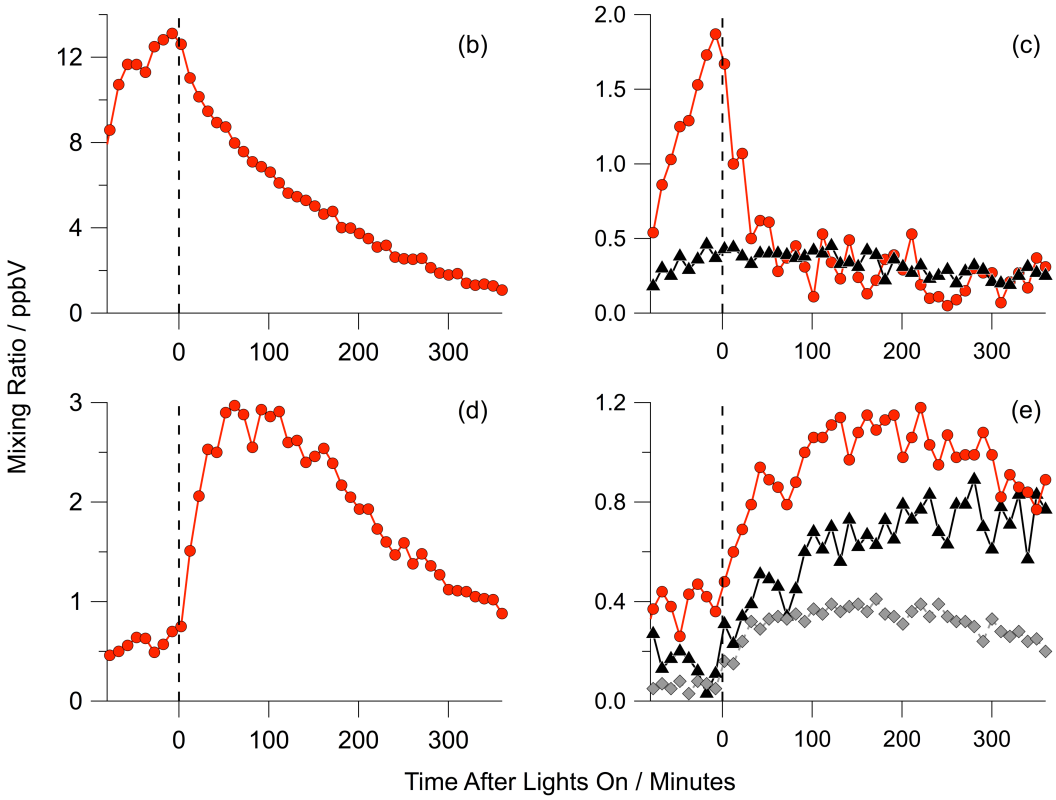

1544

1545 Figure 2: Temporal evolution of a series of isoprenoid "precursor" compounds and
1546 their oxidation products, as observed in the main reaction chamber during an example
1547 *Betula pendula* experiment (07/0709). The top panel (a) shows the entire experiment
1548 process in terms of monoterpene evolution, from background (BG) and plant chamber
1549 (PC) measurements, to reaction chamber (RC) fill and the main photooxidation
1550 experiment within the reaction chamber. Figure (b) shows monoterpene evolution, (c)
1551 shows sequiterpenes (red circles and lines) and camphore (black triangles and lines),
1552 (d) $\Sigma(I_{111}, I_{93})$ and (e) the primary ketone (*m/z* 139) (red circles and lines), primary
1553 keto-aldehyde (*m/z* 107 + 151 + 169) (black triangles and lines) and MVK + MACR
1554 (*m/z* 71) (grey diamonds and dashed line).

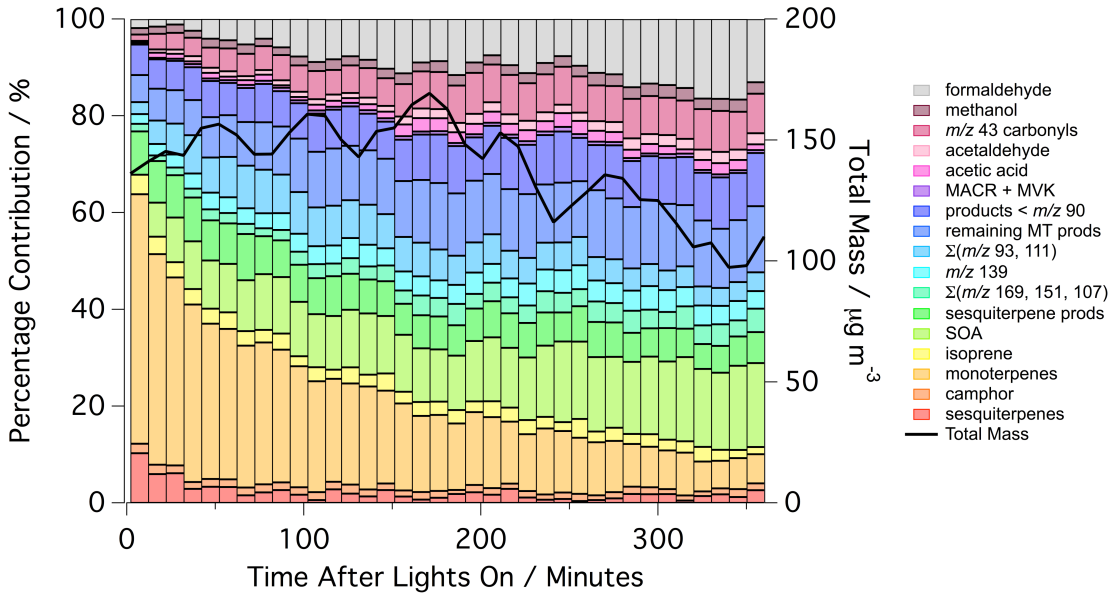

Figure 3: Evolution of measured mass through the *Betula pendula* system (7 July 2009), showing the relative contribution of precursor compounds, oxidation products and SOA mass to total measured mass, with time (coloured bars, left axis) and total measured mass (i.e. ΣVOCs + SOA) with time (black line, right axis). Note: ammonium sulphate seed mass removed from the SOA mass concentration.

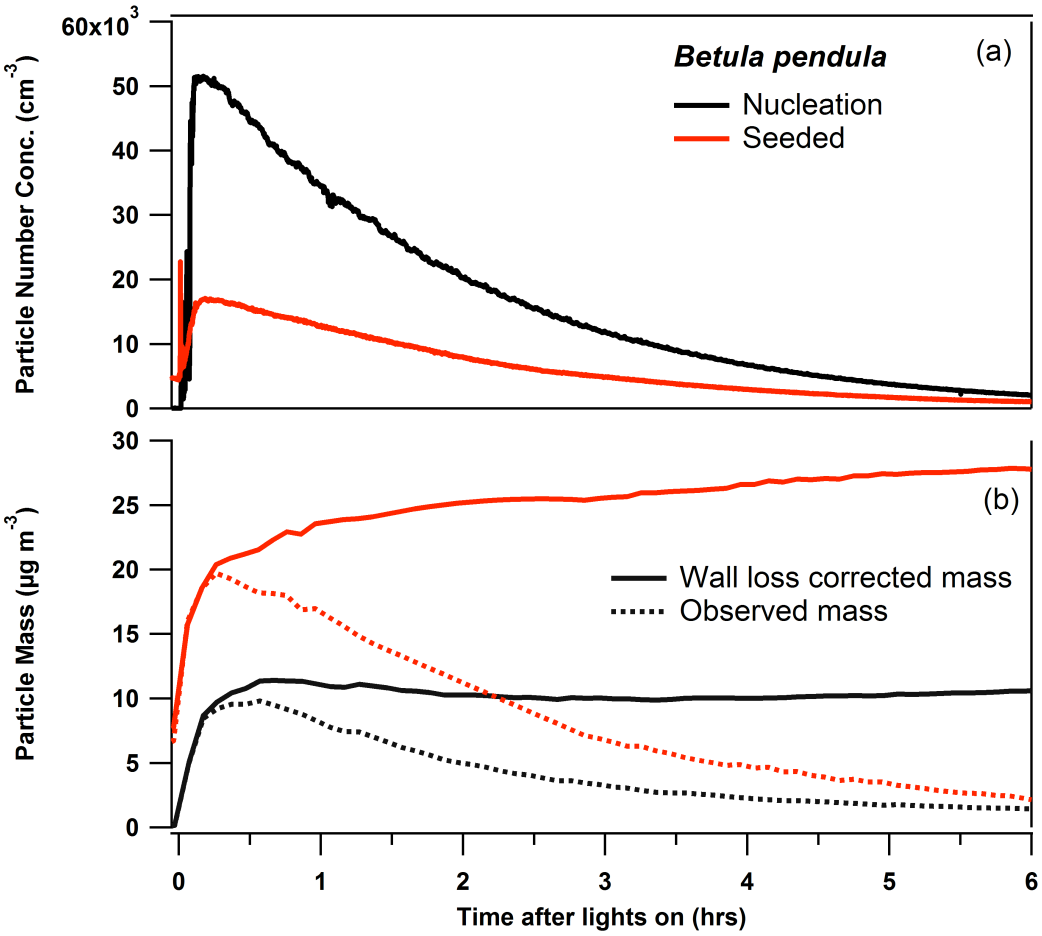

1564

1565

1566 Figure 4: Particle number and mass concentrations measured during nucleation

1567 (06/07/09) and ammonium sulphate seeded (07/07/09) *Betula pendula* experiments

1568 (a). In the bottom panel (b), both the measured (dashed lines) and the wall loss

1569 corrected (solid lines) mass concentrations are shown.

1570

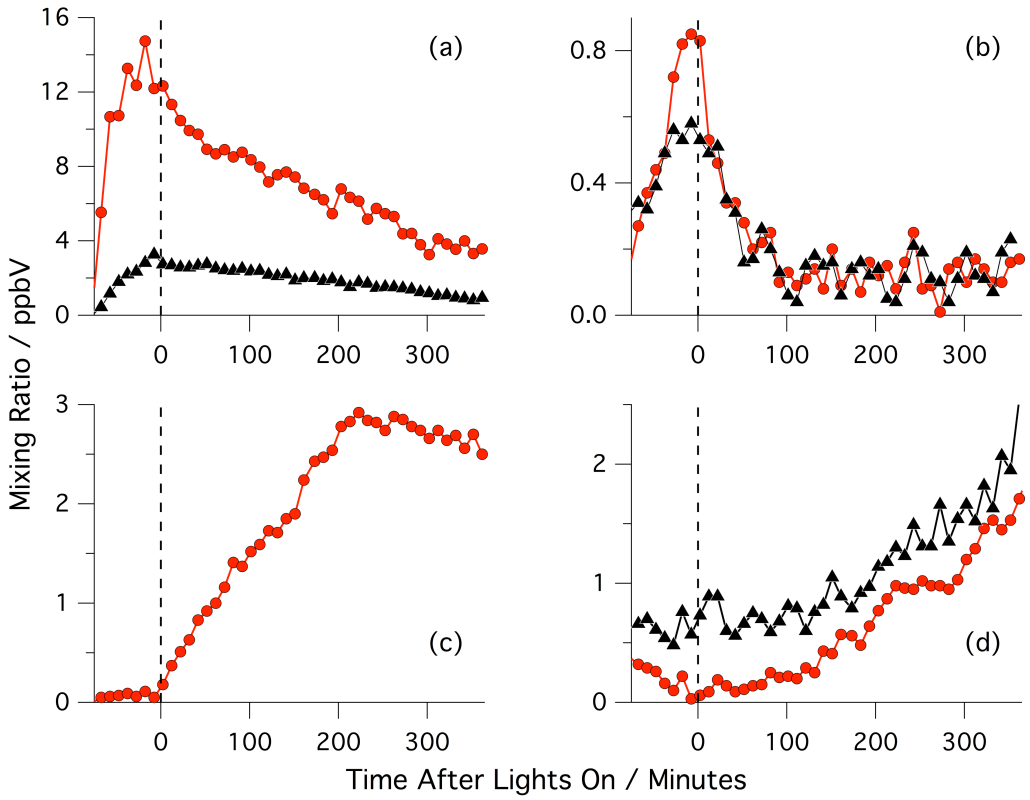

1571

1572

1573 Figure 5: Temporal evolution of a series of isoprenoid "precursor" compounds and
1574 their oxidation products, as observed in the main reaction chamber during an example
1575 *Ficus benjamina* experiment (23/06/09). Panel (a) shows isoprene (red circles and
1576 lines) and camphore (black triangles and lines) evolution, (b) shows monoterpenes
1577 (red circles and lines) and sesquiterpenes (black triangles and lines), (c) MVK +
1578 MACR (*m/z* 71) and (d) Σ(monoterpene products) (black triangles and lines) and
1579 Σ(non MVK+MACR isoprene products) (red circles and lines)

1580

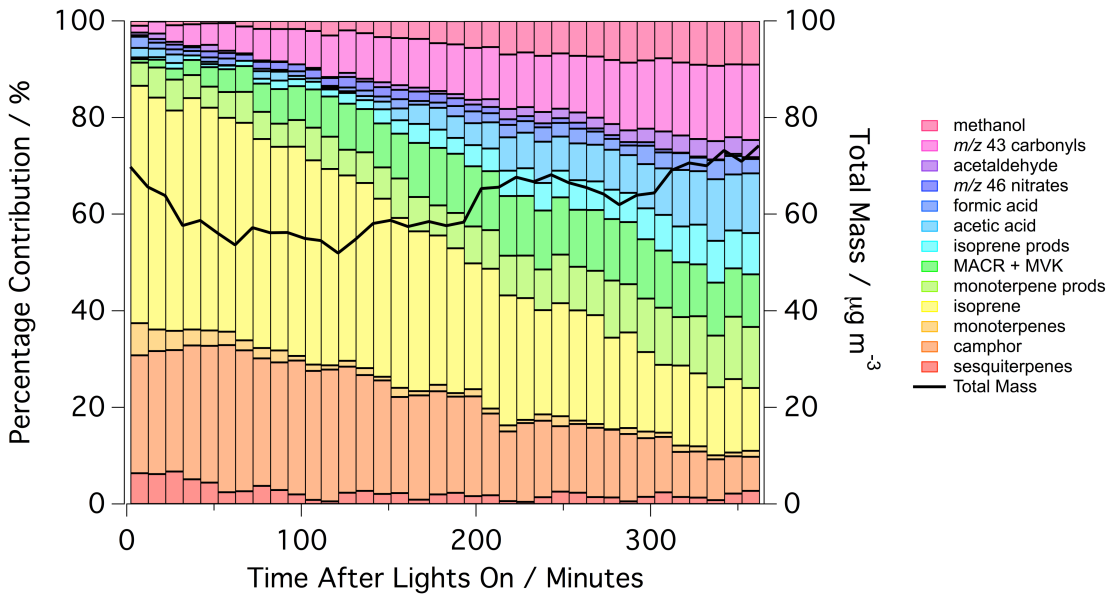

1581

1582

1583 Figure 6: Evolution of measured mass through the *Ficus benjamina* system (23 June

1584 2009), showing the relative contribution of precursor compounds and oxidation

1585 products to total measured mass, with time (coloured bars, left axis) and total

1586 measured mass (i.e. ΣVOCs + SOA) with time (black line, right axis).

1587

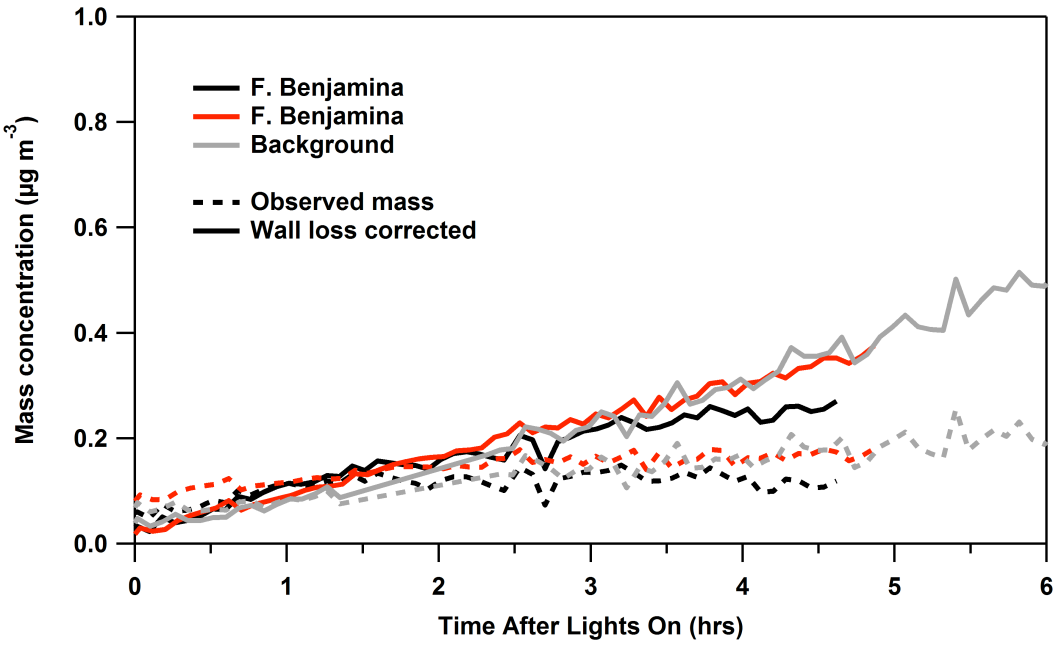

1588

1589

1590 Figure 7: Observed and wall loss corrected particle mass concentrations during un-
1591 seeded *Ficus benjamina* (22/06/09, 23/06/09) and chamber background (26/06/09)
1592 experiments. The reaction chamber was filled with plant chamber air over a period of
1593 1 – 1.5 hours. Chamber filling was carried out in the dark. Ozone was added
1594 immediately prior to lights on. Time begins at the point at which the reaction chamber
1595 was illuminated, then increments in hours after lights on.

1596

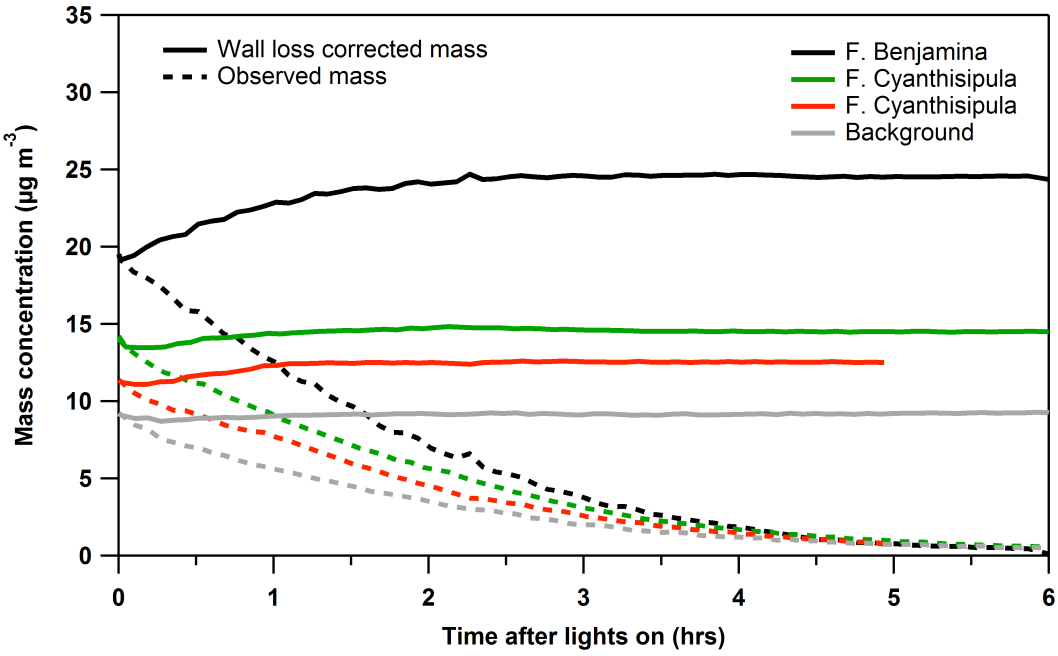

1597

1598

1599 Figure 8: Observed and wall loss corrected particle mass concentrations during
1600 ammonium sulphate seeded *Ficus benjamina* (15/07/09), *Ficus cyathistipula*
1601 (30/06/09, 02/07/09) and chamber background (03/07/09) experiments. Ozone and
1602 ammonium sulphate seed were added immediately prior to lights on.

1603

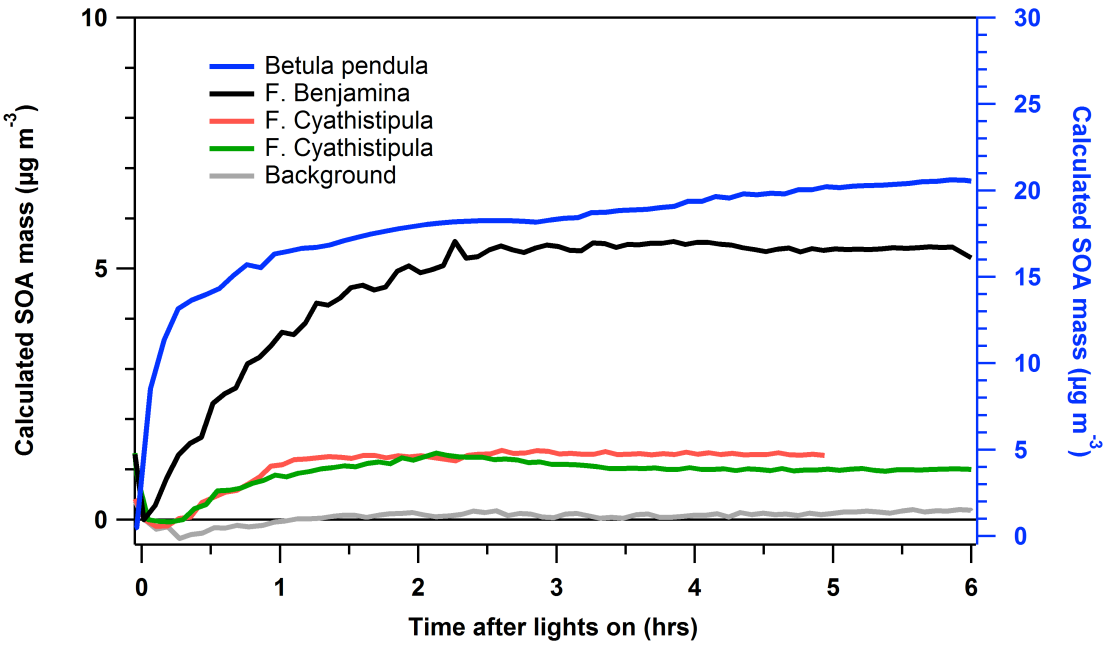

1604

1605

1606 Figure 9: Calculated SOA mass concentrations during ammonium sulphate seeded

1607 experiments for *Betula pendula* (07/07/09), *Ficus benjamina* (15/07/09) and *Ficus*

1608 *cyathistipula* (30/06/09, 02/07/09). See text for details.

1609

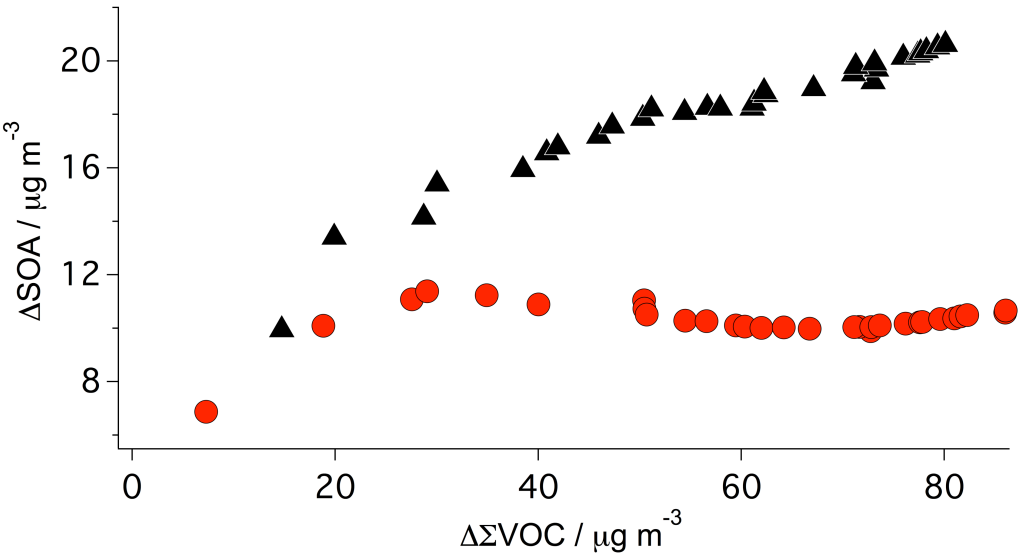

1610

1611

1612 Figure 10: Time dependent growth curves for two typical *Betula pendula* experiments
1613 (red circles- nucleation experiment on 06/07/09 and black triangles- ammonium
1614 sulphate seeded experiment on 07/07/09), showing SOA growth behaviour with
1615 respect to consumption of the VOC precursors.

1616

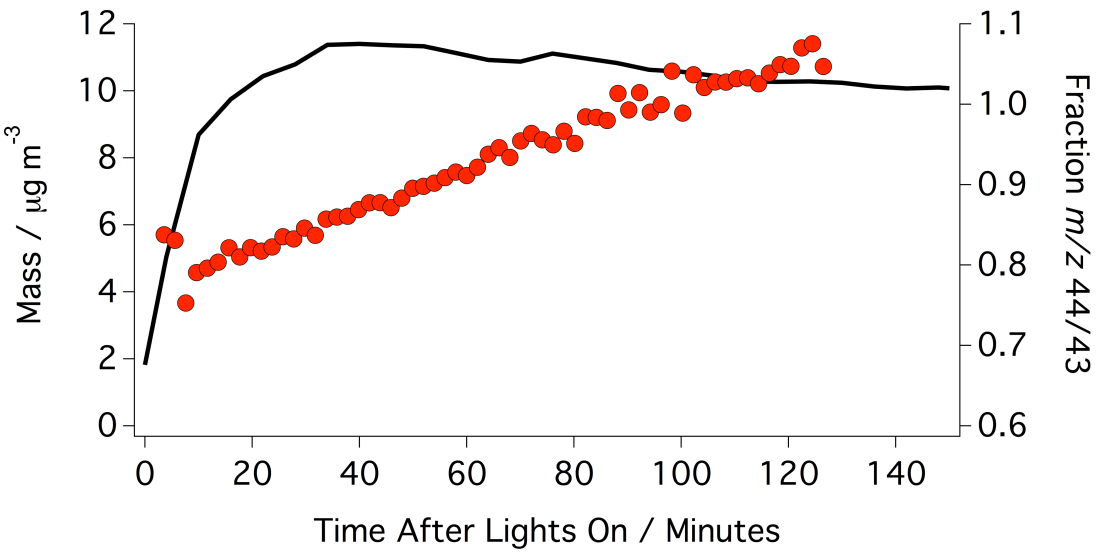

1617

1618

1619 Figure 11: Temporal evolution of the *m/z* 44/43 ratio (red circles) during a typical

1620 *Betula pendula* experiment (06/07/09) and wall loss corrected SOA mass (black line);

1621 demonstrating the increase in oxygenated content of the SOA as the air matrix begins

1622 to age.

1623

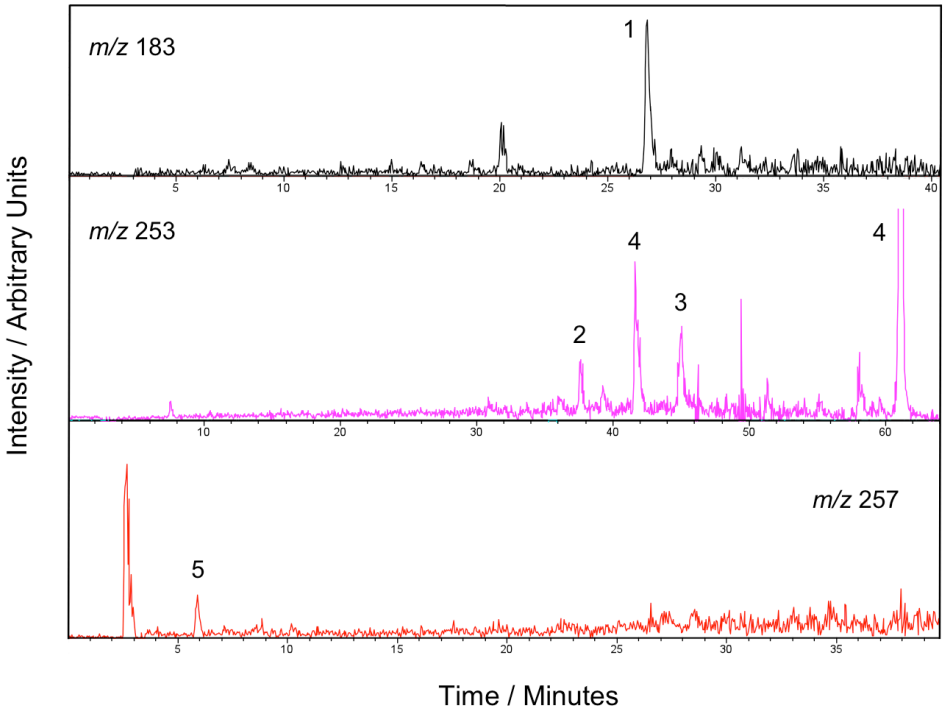

1624

1625 Figure 12: LC-MS^2 selected ion chromatograms derived from the off-line analysis of
1626 SOA collected on filters at the conclusion of a typical *Betula pendula* experiment
1627 (07/07/2009). Notes: Upper; *m/z* 183 = MW 184, 1 = cis-pinonic acid. Middle; *m/z*
1628 253 = MW 254, 2 = β-nocaryophyllonic acid, 3 = β-caryophyllinic acid, 4 = similar
1629 to sesquiterpene SOA. Lower; *m/z* 257 = MW 118 [2*[M-H] + Na]$^-$, also seen in
1630 myrcene SOA, with same MS^2 spectra.